

LEGENDRE POLYNOMIALS AND THEIR USE FOR KARHUNEN–LOÈVE EXPANSION

MICHAL BÉREŠ

Dedicated to the memory of Prof. Radim Blaheta — an inspiring teacher, generous mentor, and truly kind person.

ABSTRACT. This paper makes two main contributions. First, we present a pedagogical review of the derivation of the three-term recurrence relation for Legendre polynomials, without relying on the classical Legendre differential equation, Rodrigues’ formula, or generating functions. This exposition is designed to be accessible to undergraduate students.

Second, we develop a computational framework for Karhunen–Loève expansions of isotropic Gaussian random fields on hyper-rectangular domains. The framework leverages Legendre polynomials and their associated Gaussian quadrature, and it remains efficient even in higher spatial dimensions.

A covariance kernel is first approximated by a non-negative mixture of squared-exponentials, obtained via a Newton-optimized fit with a theoretically informed initialization. The resulting separable kernel enables a Legendre–Galerkin discretization in the form of a Kronecker product over single dimensions, with submatrices that exhibit even/odd parity structure. For assembly, we introduce a Duffy-type transformation followed by quadrature. These structural properties significantly reduce both memory usage and arithmetic cost compared to naive approaches. All algorithms and numerical experiments are provided in an open-source repository that reproduces every figure and table in this work.

1. INTRODUCTION

1.1. Motivation. The rapid growth of computational power has made it feasible to solve large systems of partial differential equations (PDEs) with uncertain input data. A prominent example arises in geoscience, where the hydraulic conductivity of an aquifer is often sparsely measured and must therefore be described statistically [13, 11]. Such situations call for realistic *Gaussian random fields* (GRFs), whose samples or low-rank representations can be incorporated into a downstream PDE solver. Among the available dimension-reduction tools, the Karhunen–Loève (KL) expansion is preferred because it minimizes the mean-square truncation error for any fixed number of terms [22, 15]. Unfortunately, a straightforward Galerkin

Date: July 15, 2025.

2020 Mathematics Subject Classification. 65C05, 86-08, 82-08, 65C60, 60-08.

Key words and phrases. Karhunen–Loève expansion, Legendre polynomials, squared-exponential approximation.

This work was supported by the European Union under Grant Agreement no. 101166718 (EURAD-2 project).

This article was co-funded by the European Union under the REFRESH – Research Excellence For REgion Sustainability and High-tech Industries project number CZ.10.03.01/00/22_003/0000048 via the Operational Programme Just Transition.

discretization of the KL integral operator yields dense matrices, whose assembly and eigendecomposition become computationally prohibitive in more than two spatial dimensions.

1.2. State of the Art. Polynomial–Galerkin solvers for the Fredholm eigenproblem underlying the Karhunen–Loève (KL) expansion have steadily advanced. Early convergence analyses for low-order bases [19] and benchmark comparisons of Nystrom, collocation, and finite element methods [6] identified dense matrix assembly as the primary bottleneck. Exponential accuracy with Legendre spectral elements [24], multilevel correction strategies [34], sparsity-oriented Chebyshev and Haar variants [21, 3], and isogeometric formulations enabling matrix-free tensor contractions [25, 23] have all reduced computational costs in specific settings. A discontinuous Legendre approach further exploits block-diagonal mass matrices [4]. Yet, to the best of our knowledge, no existing method simultaneously leverages

- (i) the separability introduced by non-negative squared-exponential fits of isotropic covariances,
- (ii) the Kronecker structure arising from separability, hyper-rectangular domains, and tensor-product bases,
- (iii) and the even/odd parity symmetry of Legendre modes, which leads to block-diagonal matrices.

The framework developed in this paper unifies these three ingredients: a squared-exponential kernel approximation feeds a tensor-product Legendre–Galerkin discretisation; parity splits the spectrum into independent blocks; and each block is stored and applied as a Kronecker product. This synergy reduces memory and arithmetic requirements by orders of magnitude while preserving the KL expansion’s optimal mean-square truncation error.

1.3. Contributions. This paper addresses the bottleneck caused by dense matrices arising from Galerkin discretisation and aims to keep the mathematics accessible to a broad audience. It makes two contributions:

- (1) *Elementary derivation of Legendre polynomials.* In Section 2, we re-derive the three-term recurrence relation for Legendre orthogonal polynomials without invoking the Legendre differential equation, Rodrigues’ formula, or generating functions. The exposition relies solely on elementary linear algebra and mathematical analysis, making it suitable for undergraduates.
- (2) *Efficient KL framework for isotropic GRFs.* Sections 3–5 develop a pipeline for KL expansions on D -dimensional hyper-rectangles. The key ingredients are:
 - a covariance kernel fitted by a **non-negative** mixture of squared-exponentials (Section 4), obtained via a Newton solver with an initial guess guided by a Gaussian quadrature interpretation;
 - a Legendre–Galerkin discretisation that exploits the separability of the fitted kernel to form a Kronecker sum of one-dimensional blocks (Section 5.2);
 - a tensor-structured assembly whose submatrices decompose into even/odd parity blocks and are evaluated stably using a Duffy-type quadrature (Sections 5.3–5.4).

Together, these components significantly reduce both the memory footprint and the computational cost of computing the KL decomposition.

This paper builds upon and extends our earlier studies [7, 8], which demonstrated the suitability of a tensor-product Legendre–Galerkin discretisation for the KL decomposition of higher-dimensional fields. Compared to previous work, we enhance all aspects of the computational pipeline and provide theoretical references to support the foundations of the numerical approximation.

1.4. Reproducibility. All code implementing the functionality described in this paper, as well as all scripts required to reproduce the figures, tables, and numerical experiments, are available in a public repository at https://github.com/Beremi/KL_decomposition.

2. DERIVATION OF LEGENDRE POLYNOMIALS AND CORRESPONDING QUADRATURE RULE

This section introduces the basic theory of orthogonal polynomials and re-derives the classical *three-term recurrence relation* for Legendre polynomials. The approach taken—particularly in deriving polynomial norms—prioritizes accessibility, making it potentially suitable for undergraduate students by relying primarily on recurrence relations, rather than more advanced techniques such as the Legendre differential equation, Rodrigues’ formula, or generating functions (see, e.g., [31]).

We begin with the three-term recurrence for monic polynomials, and then use it to derive the recurrence for normalized polynomials in Subsection 2.2.1 and for classical Legendre polynomials in Subsection 2.2.2.

In Subsection 2.3, we briefly recall the connection between the Gauss quadrature rule and orthogonal polynomials in the context of efficient quadrature computation, as introduced in [18]. The recurrence relation—specifically for normalized polynomials—as well as the quadrature rule, will be used later for approximating the KL decomposition.

2.1. Preliminaries.

Definition 2.1 (Positive measure [31, 9]). Let $d\lambda(t)$ be a measure on an interval $[a, b]$ (where $a \in \mathbb{R} \cup \{-\infty\}$, $b \in \mathbb{R} \cup \{\infty\}$, and $a < b$), such that the bilinear form

$$\langle f, g \rangle_{d\lambda} = \int_a^b f(t)g(t) d\lambda(t)$$

defines an inner product on the space of real polynomials. Such a measure is called *positive*.

For a positive measure, the moments $\mu_k = \int_a^b t^k d\lambda(t)$ exist for all $k \geq 0$.

Definition 2.2 (Monic polynomials). A polynomial $p(t)$ of degree k is called *monic* if the coefficient of its highest-degree term (t^k) is equal to 1. That is,

$$p(t) = t^k + c_{k-1}t^{k-1} + \cdots + c_1t + c_0.$$

We will denote a monic polynomial of degree k by P_k^M .

2.2. Three-Term Recurrence of Legendre Polynomials. A fundamental property of orthogonal polynomials generated by a positive measure and the corresponding integral inner product is that they satisfy a three-term recurrence relation.

Theorem 2.3 ([31, 9, 14]). *Let $\pi_k(t)$, $k = 0, 1, 2, \dots$, be the sequence of monic orthogonal polynomials with respect to the positive measure $d\lambda$ on $[a, b]$. Then, they satisfy the recurrence relation:*

$$\begin{aligned}\pi_{k+1}(t) &= (t - \alpha_k)\pi_k(t) - \beta_k\pi_{k-1}(t), \quad k = 0, 1, 2, \dots, \\ \pi_{-1}(t) &\equiv 0, \quad \pi_0(t) \equiv 1,\end{aligned}$$

where the coefficients are given by

$$\begin{aligned}\alpha_k &= \frac{\langle t\pi_k, \pi_k \rangle_{d\lambda}}{\langle \pi_k, \pi_k \rangle_{d\lambda}} = \frac{\langle t\pi_k, \pi_k \rangle_{d\lambda}}{\|\pi_k\|_{d\lambda}^2}, \quad k = 0, 1, 2, \dots, \\ \beta_0 &= 0, \\ \beta_k &= \frac{\langle \pi_k, \pi_k \rangle_{d\lambda}}{\langle \pi_{k-1}, \pi_{k-1} \rangle_{d\lambda}} = \frac{\|\pi_k\|_{d\lambda}^2}{\|\pi_{k-1}\|_{d\lambda}^2}, \quad k = 1, 2, \dots\end{aligned}$$

We now restrict our attention to Legendre polynomials, which are orthogonal with respect to the measure $d\lambda(t) = dt$ on the interval $[-1, 1]$. The corresponding inner product is given by:

$$\langle f, g \rangle = \int_{-1}^1 f(t)g(t) dt.$$

Theorem 2.4. *For the monic Legendre polynomials $\{\pi_k(t)\}_{k=0}^\infty$, orthogonal with respect to the inner product $\langle f, g \rangle = \int_{-1}^1 f(t)g(t) dt$, the recurrence coefficients α_k are all zero:*

$$\alpha_k = \frac{\langle t\pi_k, \pi_k \rangle}{\|\pi_k\|^2} = 0, \quad k = 0, 1, 2, \dots$$

Furthermore, the monic Legendre polynomials exhibit alternating parity: $\pi_k(-t) = (-1)^k \pi_k(t)$. Specifically, $\pi_k(t)$ is an even function if k is even, and an odd function if k is odd.

Proof. We prove that $\alpha_k = 0$ and the parity property simultaneously by induction.

- $k = 0$: $\pi_0(t) = 1$, which is an even function.

$$\langle t\pi_0, \pi_0 \rangle = \int_{-1}^1 t dt = \left[\frac{t^2}{2} \right]_{-1}^1 = \frac{1}{2} - \frac{1}{2} = 0.$$

Since the numerator is zero and $\|\pi_0\|^2 = \int_{-1}^1 1^2 dt = 2 > 0$, we have $\alpha_0 = 0$.

- $k = 1$: Using Theorem 2.3 with $k = 0$:

$$\pi_1(t) = (t - \alpha_0)\pi_0(t) - \beta_0\pi_{-1}(t) = (t - 0)(1) - 0 = t.$$

Thus, $\pi_1(t) = t$ is an odd function. Now compute α_1 :

$$\langle t\pi_1, \pi_1 \rangle = \int_{-1}^1 t^3 dt = \left[\frac{t^4}{4} \right]_{-1}^1 = \frac{1}{4} - \frac{1}{4} = 0.$$

Since $\|\pi_1\|^2 = \int_{-1}^1 t^2 dt = \frac{2}{3} > 0$, we have $\alpha_1 = 0$.

- **Inductive step:** Assume $\alpha_i = 0$ and $\pi_i(-t) = (-1)^i \pi_i(t)$ for all $0 \leq i \leq k$. We need to show $\alpha_{k+1} = 0$ and that $\pi_{k+1}(-t) = (-1)^{k+1} \pi_{k+1}(t)$.

From the recurrence (using $\alpha_k = 0$),

$$\pi_{k+1}(t) = t\pi_k(t) - \beta_k\pi_{k-1}(t), \quad k \geq 1.$$

Applying the inductive hypothesis:

$$\begin{aligned}\pi_{k+1}(-t) &= (-t)\pi_k(-t) - \beta_k\pi_{k-1}(-t) \\ &= (-t)(-1)^k\pi_k(t) - \beta_k(-1)^{k-1}\pi_{k-1}(t) \\ &= (-1)^{k+1}(t\pi_k(t) - \beta_k\pi_{k-1}(t)) = (-1)^{k+1}\pi_{k+1}(t).\end{aligned}$$

To compute α_{k+1} , consider:

$$\langle t\pi_{k+1}, \pi_{k+1} \rangle = \int_{-1}^1 t[\pi_{k+1}(t)]^2 dt.$$

The integrand $t[\pi_{k+1}(t)]^2$ is odd: t is odd, $[\pi_{k+1}(t)]^2$ is even. Thus, the integral over the symmetric interval $[-1, 1]$ vanishes:

$$\int_{-1}^1 t[\pi_{k+1}(t)]^2 dt = 0.$$

Since $\|\pi_{k+1}\|^2 > 0$ (as $\pi_{k+1}(t) \neq 0$ for all $t \in [-1, 1]$), we conclude that $\alpha_{k+1} = 0$. □

Lemma 2.5. *Given $a_1 = 1$ and the recurrence relation for $k \geq 2$:*

$$a_k = 1 - \frac{2k-3}{2k-1}a_{k-1},$$

the explicit formula for a_k is

$$a_k = \frac{k}{2k-1}, \quad \text{for } k \geq 1.$$

Proof. We prove this by induction.

- **Base case ($k = 1$):**

$$a_1 = \frac{1}{2(1)-1} = \frac{1}{1} = 1.$$

- **Inductive step:** Assume $a_{k-1} = \frac{k-1}{2(k-1)-1} = \frac{k-1}{2k-3}$ holds for some $k \geq 2$. Substituting into the recurrence relation:

$$\begin{aligned}a_k &= 1 - \frac{2k-3}{2k-1}a_{k-1} = 1 - \frac{2k-3}{2k-1} \left(\frac{k-1}{2k-3} \right) = 1 - \frac{k-1}{2k-1} \\ &= \frac{2k-1-(k-1)}{2k-1} = \frac{2k-1-k+1}{2k-1} = \frac{k}{2k-1}.\end{aligned}$$

□

Lemma 2.6. *Let $\{\pi_k(t)\}_{k=0}^\infty$ be a sequence of monic orthogonal polynomials with respect to an inner product $\langle \cdot, \cdot \rangle_{d\lambda}$ (with corresponding norm $\|\cdot\|_{d\lambda}$). For any $k \geq 0$, if $P_k^M(t)$ is any monic polynomial of degree k , then*

$$\langle \pi_k, P_k^M \rangle_{d\lambda} = \|\pi_k\|_{d\lambda}^2.$$

Proof. Let $P_k^M(t)$ be an arbitrary monic polynomial of degree k . We can express $P_k^M(t)$ in the orthogonal basis $\{\pi_k(t)\}_{k=0}^\infty$ as

$$P_k^M(t) = \pi_k(t) + \sum_{j=0}^{k-1} c_j \pi_j(t).$$

By linearity of the inner product, we have

$$\langle \pi_k, P_k^M \rangle_{d\lambda} = \langle \pi_k, \pi_k \rangle_{d\lambda} + \sum_{j=0}^{k-1} c_j \langle \pi_k, \pi_j \rangle_{d\lambda}.$$

Since the polynomials are orthogonal, $\langle \pi_k, \pi_j \rangle_{d\lambda} = 0$ for $k \neq j$. Thus,

$$\langle \pi_k, P_k^M \rangle_{d\lambda} = \|\pi_k\|_{d\lambda}^2.$$

□

Theorem 2.7 ([1, 31]). *For the monic Legendre polynomials $\pi_k(t)$, the following hold:*

(1) **Relationship between norm and value at $t = 1$:**

$$(2.1) \quad \|\pi_k\|^2 = \frac{2\pi_k^2(1)}{2k+1}, \quad k \geq 0.$$

(2) **Explicit value at $t = 1$:**

$$(2.2) \quad \pi_k(1) = \frac{2^k (k!)^2}{(2k)!}, \quad k \geq 0.$$

(3) **Explicit squared norm:**

$$(2.3) \quad \|\pi_k\|^2 = \frac{2^{2k+1} (k!)^4}{(2k+1) ((2k)!)^2}, \quad k \geq 0.$$

Proof. We first derive the relationship (2.1), then find the explicit formula for $\pi_k(1)$ (2.2), and finally combine them to obtain the explicit norm (2.3).

Part 1: Relationship between $\|\pi_k\|^2$ and $\pi_k(1)$. We apply integration by parts to $\|\pi_k\|^2$:

$$(2.4) \quad \|\pi_k\|^2 = \int_{-1}^1 \pi_k(t)^2 dt = [t\pi_k^2(t)]_{-1}^1 - \int_{-1}^1 t \cdot 2\pi_k(t)\pi_k'(t) dt.$$

From Theorem 2.4, we know that $\pi_k(-t) = (-1)^k \pi_k(t)$, implying $\pi_k^2(-1) = \pi_k^2(1)$. The boundary term evaluates to:

$$[t\pi_k^2(t)]_{-1}^1 = \pi_k^2(1) + \pi_k^2(1) = 2\pi_k^2(1).$$

If $k = 0$, then

$$\int_{-1}^1 t \cdot 2\pi_k(t)\pi_k'(t) dt = 0,$$

so $\|\pi_k\|^2 = 2\pi_k^2(1)$. If $k > 0$, then $t\pi_k'(t) = kP_k^M(t)$ for a monic polynomial $P_k^M(t)$ of degree k , since the leading term of π_k' is kt^{k-1} . By Lemma 2.6,

$$\int_{-1}^1 2t\pi_k(t)\pi_k'(t) dt = 2k \int_{-1}^1 \pi_k(t)P_k^M(t) dt = 2k\|\pi_k\|^2.$$

Substituting into (2.4), we obtain:

$$(2.5) \quad \|\pi_k\|^2 = 2\pi_k^2(1) - 2k\|\pi_k\|^2, \quad \forall k \geq 0.$$

Solving gives:

$$\|\pi_k\|^2 = \frac{2\pi_k^2(1)}{2k+1}, \quad \forall k \geq 0.$$

Part 2: Explicit formula for $\pi_k(1)$. We know that $\pi_0(t) = 1$ and $\pi_1(t) = t$, so $\pi_0(1) = \pi_1(1) = 1$. From the recurrence relation at $t = 1$:

$$\pi_k(1) = \pi_{k-1}(1) - \beta_{k-1}\pi_{k-2}(1), \quad \forall k \geq 2,$$

where $\beta_{k-1} = \frac{\|\pi_{k-1}\|^2}{\|\pi_{k-2}\|^2}$ (Theorem 2.3). Using the result from Part 1:

$$\|\pi_j\|^2 = \frac{2\pi_j^2(1)}{2j+1}.$$

We substitute this into the recurrence:

$$\pi_k(1) = \pi_{k-1}(1) - \frac{\frac{2\pi_{k-1}^2(1)}{2k-1}}{\frac{2\pi_{k-2}^2(1)}{2k-3}} \pi_{k-2}(1) = \pi_{k-1}(1) - \frac{2k-3}{2k-1} \cdot \frac{2\pi_{k-1}^2(1)}{2\pi_{k-2}(1)}.$$

Letting $a_k = \pi_k(1)/\pi_{k-1}(1)$, we derive the recurrence:

$$a_k = 1 - \frac{2k-3}{2k-1} a_{k-1}, \quad k \geq 2,$$

with $a_1 = 1$. By Lemma 2.5, this gives:

$$a_k = \frac{k}{2k-1}.$$

Hence,

$$\pi_k(1) = \prod_{i=1}^k a_i = \prod_{i=1}^k \frac{i}{2i-1} = \frac{k!}{1 \cdot 3 \cdot 5 \cdots (2k-1)}.$$

Using the identity

$$1 \cdot 3 \cdot 5 \cdots (2k-1) = \frac{1 \cdot 2 \cdot 3 \cdot 4 \cdot 5 \cdot 6 \cdots (2k)}{2 \cdot 4 \cdot 6 \cdots (2k)} = \frac{(2k)!}{2^k k!},$$

we obtain:

$$\pi_k(1) = \frac{k!}{\frac{(2k)!}{2^k k!}} = \frac{2^k (k!)^2}{(2k)!}, \quad k \geq 0.$$

Part 3: Explicit squared norm. Substituting (2.2) into (2.1) gives:

$$\|\pi_k\|^2 = \frac{2}{2k+1} \left(\frac{2^k (k!)^2}{(2k)!} \right)^2.$$

Simplifying:

$$\|\pi_k\|^2 = \frac{2}{2k+1} \cdot \frac{2^{2k} (k!)^4}{((2k)!)^2} = \frac{2^{2k+1} (k!)^4}{(2k+1)((2k)!)^2}, \quad k \geq 0.$$

□

Theorem 2.8. *For the monic Legendre polynomials, the recurrence coefficient β_k for $k \geq 1$ is given by*

$$\beta_k = \frac{k^2}{4k^2 - 1}.$$

Proof. Starting from the definition in Theorem 2.3:

$$\beta_k = \frac{\|\pi_k\|^2}{\|\pi_{k-1}\|^2}, \quad k \geq 1.$$

Using the result from Theorem 2.7:

$$\|\pi_k\|^2 = \frac{2^{2k+1}(k!)^4}{(2k+1)((2k)!)^2},$$

and for $k-1$:

$$\|\pi_{k-1}\|^2 = \frac{2^{2k-1}((k-1)!)^4}{(2k-1)((2k-2)!)^2}.$$

Now compute the ratio:

$$\begin{aligned} \beta_k &= \frac{\|\pi_k\|^2}{\|\pi_{k-1}\|^2} = \frac{\frac{2^{2k+1}(k!)^4}{(2k+1)((2k)!)^2}}{\frac{2^{2k-1}((k-1)!)^4}{(2k-1)((2k-2)!)^2}} = \frac{2^{2k+1}(k!)^4}{(2k+1)((2k)!)^2} \cdot \frac{(2k-1)((2k-2)!)^2}{2^{2k-1}((k-1)!)^4} \\ &= \frac{2^{2k+1}}{2^{2k-1}} \cdot \frac{(k!)^4}{((k-1)!)^4} \cdot \frac{2k-1}{2k+1} \cdot \frac{((2k-2)!)^2}{((2k)!)^2} \\ &= 4 \cdot k^4 \cdot \frac{2k-1}{2k+1} \cdot \frac{1}{(2k)^2(2k-1)^2} = \frac{k^2}{4k^2-1}. \end{aligned}$$

□

Corollary 2.9 (Recurrence for Monic Legendre Polynomials). *The three-term recurrence relation for the monic Legendre polynomials $\pi_k(t)$ is*

$$\pi_{k+1}(t) = t\pi_k(t) - \frac{k^2}{4k^2-1}\pi_{k-1}(t), \quad k = 1, 2, \dots$$

with initial conditions $\pi_0(t) = 1$ and $\pi_1(t) = t$.

2.2.1. *Three-term recurrence relation for normalized Legendre polynomials.* Orthonormal polynomials $\tilde{\pi}_k(t)$ are obtained by normalizing the monic orthogonal polynomials:

$$\tilde{\pi}_k(t) = \frac{\pi_k(t)}{\|\pi_k\|_{d\lambda}}, \quad \text{so that } \langle \tilde{\pi}_k, \tilde{\pi}_j \rangle_{d\lambda} = \delta_{kj}.$$

They also satisfy a three-term recurrence relation, which can be derived from the recurrence for the monic polynomials.

Theorem 2.10 (Orthonormal Legendre polynomials). *The orthonormal Legendre polynomials $\tilde{\pi}_k(t)$ satisfy the three-term recurrence relation:*

$$(2.6) \quad \tilde{\pi}_{k+1}(t) = \sqrt{4 - \frac{1}{(k+1)^2}} \left(t\tilde{\pi}_k(t) - \frac{1}{\sqrt{4 - \frac{1}{k^2}}} \tilde{\pi}_{k-1}(t) \right), \quad k = 1, 2, \dots$$

with initial conditions $\tilde{\pi}_0(t) = 1/\|\pi_0\| = 1/\sqrt{2}$ and $\tilde{\pi}_1(t) = t/\|\pi_1\| = \sqrt{\frac{3}{2}}t$.

Proof. Let

$$a_k := \|\pi_k\| \implies \tilde{\pi}_k(t) = \frac{\pi_k(t)}{a_k}, \quad k \geq 0.$$

The monic Legendre relation (Corollary 2.9) divided by a_{k+1} , reads

$$(2.7) \quad \tilde{\pi}_{k+1}(t) = \frac{a_k}{a_{k+1}} \left(t\tilde{\pi}_k(t) - \frac{k^2}{4k^2-1} \cdot \frac{a_{k-1}}{a_k} \tilde{\pi}_{k-1}(t) \right), \quad k \geq 1.$$

From the explicit norm formula $a_k^2 = \frac{2^{2k+1}(k!)^4}{(2k+1)((2k)!)^2}$ (Theorem 2.7) one finds

$$\begin{aligned} \frac{a_k^2}{a_{k+1}^2} &= \frac{2^{2k+1}(k!)^4}{(2k+1)((2k)!)^2} \cdot \frac{(2k+3)((2k+2)!)^2}{2^{2k+3}((k+1)!)^4} = \frac{4(k+1)^2(2k+1)(2k+3)}{4(k+1)^4} \\ &= \frac{4k^2+8k+3}{(k+1)^2} = 4 - \frac{1}{(k+1)^2}, \\ \frac{a_{k-1}^2}{a_{k+1}^2} &= \frac{a_{k-1}^2}{a_k^2} \cdot \frac{a_k^2}{a_{k+1}^2}. \end{aligned}$$

Hence

$$\begin{aligned} \frac{a_k}{a_{k+1}} &= \sqrt{4 - \frac{1}{(k+1)^2}}, \\ \frac{k^2}{4k^2-1} \frac{a_{k-1}}{a_k} &= \frac{k^2}{4k^2-1} \sqrt{4 - \frac{1}{k^2}} = \frac{k^2}{4k^2-1} \sqrt{\frac{4k^2-1}{k^2}} = \frac{k\sqrt{4k^2-1}}{4k^2-1} = \frac{1}{\sqrt{4 - \frac{1}{k^2}}}. \end{aligned}$$

Substituting the two ratios gives

$$\tilde{\pi}_{k+1}(t) = \sqrt{4 - \frac{1}{(k+1)^2}} \left(t \tilde{\pi}_k(t) - \frac{1}{\sqrt{4 - \frac{1}{k^2}}} \tilde{\pi}_{k-1}(t) \right), \quad k \geq 1,$$

which is exactly (2.6). The initial values follow from $\tilde{\pi}_0(t) = \pi_0(t)/a_0 = 1/\sqrt{2}$ and $\tilde{\pi}_1(t) = t/a_1 = t\sqrt{3}/2$. \square

2.2.2. Three-term recurrence relation for classical Legendre polynomials. We define the *classical* Legendre polynomials P_k by

$$(2.8) \quad d_k P_k(t) = \pi_k(t) \implies P_k(1) = 1, \quad k \geq 0,$$

where

$$(2.9) \quad d_k := \pi_k(1) = \frac{2^k(k!)^2}{(2k)!}, \quad k \geq 0,$$

see Theorem 2.7.

Theorem 2.11. *For every $k \geq 1$ the polynomials defined in (2.8) satisfy*

$$(k+1)P_{k+1}(t) = (2k+1)tP_k(t) - kP_{k-1}(t), \quad P_0(t) = 1, \quad P_1(t) = t.$$

Proof. We start the proof by substituting (2.8) into the *monic* Legendre three-term recurrence (Corollary 2.9):

$$d_{k+1}P_{k+1}(t) = t d_k P_k(t) - \frac{k^2}{4k^2-1} d_{k-1} P_{k-1}(t).$$

Dividing by d_{k+1} gives

$$P_{k+1}(t) = \frac{d_k}{d_{k+1}} t P_k(t) - \frac{k^2}{4k^2-1} \frac{d_{k-1}}{d_{k+1}} P_{k-1}(t).$$

Using (2.9) one finds

$$\frac{d_k}{d_{k+1}} = \frac{(2k+1)(2k+2)}{2(k+1)^2} = \frac{2k+1}{k+1}, \quad \frac{d_{k-1}}{d_{k+1}} = \frac{(2k+1)(2k-1)}{k(k+1)}.$$

(The first equality comes from

$$\frac{(2(k+1))!}{2^{k+1}((k+1)!)^2} = \frac{(2k)!}{2^k(k!)^2} \frac{(2k+1)(2k+2)}{2(k+1)^2},$$

and multiplying it by $\frac{2k(2k-1)}{2k^2}$ yields the second.)

Because

$$\frac{k^2}{4k^2-1} \frac{d_{k-1}}{d_{k+1}} = \frac{k^2}{(2k+1)(2k-1)} \frac{(2k+1)(2k-1)}{k(k+1)} = \frac{k}{k+1},$$

we obtain

$$P_{k+1}(t) = \frac{2k+1}{k+1} t P_k(t) - \frac{k}{k+1} P_{k-1}(t).$$

Multiplying through by $k+1$ gives the claimed recurrence. \square

2.3. Construction of an n -Point Gaussian Quadrature Rule. Let $\{\pi_k\}_{k=0}^\infty$ be the monic orthogonal polynomials from Theorem 2.3, with recurrence coefficients $\{\alpha_k\}_{k \geq 0}$ and $\{\beta_k\}_{k \geq 1}$. Following [18], define the *Jacobi matrix*

$$J_n = \begin{pmatrix} \alpha_0 & \sqrt{\beta_1} & & \\ \sqrt{\beta_1} & \alpha_1 & \ddots & \\ & \ddots & \ddots & \sqrt{\beta_{n-1}} \\ & & \sqrt{\beta_{n-1}} & \alpha_{n-1} \end{pmatrix} \in \mathbb{R}^{n \times n},$$

which is real, symmetric, and tridiagonal. The following holds:

- The eigenvalues $\{t_i\}_{i=1}^n$ of J_n are *exactly* the nodes of the unique n -point Gaussian quadrature rule for the measure $d\lambda$ (and also the roots of π_n). That is, $\{t_i\}_{i=1}^n \subset [a, b]$, and the node sets for the n -point and $(n+1)$ -point Gaussian quadrature satisfy the alternating property [14, Thm. 1.20].
- Let $v^{(i)} = (v_1^{(i)}, \dots, v_n^{(i)})^\top$ be a *unit* eigenvector of J_n associated with t_i . Then the corresponding positive weight is

$$w_i = m_0 (v_1^{(i)})^2 > 0, \quad i = 1, \dots, n, \quad m_0 = \int_a^b d\lambda(t).$$

Because J_n is symmetric and tridiagonal, its eigenvalues and eigenvectors can be computed in $\mathcal{O}(n^2)$ flops with high relative accuracy via the implicit-shift symmetric QR algorithm, as analyzed in [17]. SciPy's implementation `eigh_tridiagonal` uses the LAPACK routines `DSTEVD` and `DSTEV`, which realize this algorithm.

3. KARHUNEN-LOÈVE EXPANSION OF STATIONARY ISOTROPIC GAUSSIAN RANDOM FIELDS

Gaussian random fields (GRFs) are fundamental tools for modeling spatially varying quantities subject to uncertainty across numerous scientific and engineering disciplines [2]. A key challenge lies in the computational representation of these infinite-dimensional objects. The Karhunen-Loève (KL) expansion provides an optimal representation in the sense that it minimizes the mean-squared truncation error for a given number of terms [22]. This chapter focuses on the KL expansion for a specific yet widely applicable class of GRFs: zero-mean, stationary, and isotropic fields defined on a D -dimensional hyper-rectangular domain $\Omega \subset \mathbb{R}^D$.

3.1. Gaussian Random Fields and Autocovariance. Let $(\mathcal{A}, \mathcal{F}, \mathbb{P})$ be a complete probability space, and let $\Omega = [a_1, b_1] \times \cdots \times [a_D, b_D] \subset \mathbb{R}^D$ be a D -dimensional closed interval (hyper-rectangle). We consider a real-valued Gaussian random field (GRF) $Z(\mathbf{x}, \omega) : \Omega \times \mathcal{A} \rightarrow \mathbb{R}$. In the following, $Z(\mathbf{x}) \sim \mathcal{N}(\mu, \sigma)$ denotes a random variable representing the behavior of the field at a specific spatial point $\mathbf{x} \in \Omega$. We assume Z has zero mean:

$$(3.1) \quad \mathbb{E}[Z(\mathbf{x})] = 0, \quad \forall \mathbf{x} \in \Omega.$$

We further assume that Z is a *second-order* random field, meaning it has finite second moments at every spatial location:

$$(3.2) \quad \mathbb{E}[Z(\mathbf{x})^2] < \infty, \quad \forall \mathbf{x} \in \Omega.$$

This condition ensures that the covariance function introduced below is well defined.

The field is characterized by its autocovariance function $C : \Omega \times \Omega \rightarrow \mathbb{R}$, defined as:

$$(3.3) \quad C(\mathbf{x}, \mathbf{y}) = \mathbb{E}[Z(\mathbf{x})Z(\mathbf{y})], \quad \forall \mathbf{x}, \mathbf{y} \in \Omega.$$

We assume Z is stationary, meaning $C(\mathbf{x}, \mathbf{y})$ depends only on the separation vector $\mathbf{x} - \mathbf{y}$:

$$(3.4) \quad C(\mathbf{x}, \mathbf{y}) = C_S(\mathbf{x} - \mathbf{y}).$$

Furthermore, we assume Z is isotropic, meaning $C_S(\mathbf{x} - \mathbf{y})$ depends only on the Euclidean norm of the separation vector, $\|\mathbf{x} - \mathbf{y}\|_2 = \sqrt{\sum_{l=1}^D (x_l - y_l)^2}$:

$$(3.5) \quad C(\mathbf{x}, \mathbf{y}) = C_I(\|\mathbf{x} - \mathbf{y}\|_2),$$

where $C_I : [0, \infty) \rightarrow \mathbb{R}$ is a positive-semidefinite function [10]. Later in this paper, we will drop the subscripts and distinguish between C , C_S , and C_I based on the type of argument.

We assume that the sample paths of Z are square-integrable over Ω , i.e., $Z(\cdot, \omega) \in L^2(\Omega)$ almost surely. This is guaranteed if the covariance function C satisfies $\int_{\Omega} C(\mathbf{x}, \mathbf{x}) d\mathbf{x} < \infty$. For stationary fields on bounded domains, $C(\mathbf{x}, \mathbf{x}) = C_I(0) = \sigma^2$ (the variance), which is finite and ensures this condition holds.

The autocovariance function defines a linear integral operator $\mathcal{C} : L^2(\Omega) \rightarrow L^2(\Omega)$:

$$(3.6) \quad (\mathcal{C}f)(\mathbf{x}) = \int_{\Omega} C(\mathbf{x}, \mathbf{y})f(\mathbf{y}) d\mathbf{y}.$$

3.2. The Karhunen-Loève Expansion Theorem. The KL expansion provides a representation of the random field $Z(\mathbf{x})$ in terms of a deterministic orthonormal basis $\{\phi_j(\mathbf{x})\}_{j=1}^{\infty}$ of $L^2(\Omega)$ and a sequence of uncorrelated random variables $\{\xi_j(\omega)\}_{j=1}^{\infty}$.

Theorem 3.1 (Karhunen-Loève [22], [15]). *Let $Z(\mathbf{x})$ be a zero-mean, second-order random field on Ω with continuous autocovariance function $C(\mathbf{x}, \mathbf{y})$, such that $Z(\cdot, \omega) \in L^2(\Omega)$ almost surely. Let $(\lambda_j, \phi_j)_{j=1}^{\infty}$ be the eigenpairs of the autocovariance operator \mathcal{C} :*

$$(3.7) \quad \mathcal{C}\phi_j = \lambda_j\phi_j, \quad \text{i.e.,} \quad \int_{\Omega} C(\mathbf{x}, \mathbf{y})\phi_j(\mathbf{y}) d\mathbf{y} = \lambda_j\phi_j(\mathbf{x}).$$

Here, $\{\phi_j\}_{j=1}^\infty$ forms an orthonormal basis for the closure of the range of \mathcal{C} (and can be extended to an orthonormal basis of $L^2(\Omega)$). Then $Z(\mathbf{x})$ admits the following expansion:

$$(3.8) \quad Z(\mathbf{x}, \omega) = \sum_{j=1}^{\infty} \sqrt{\lambda_j} \xi_j(\omega) \phi_j(\mathbf{x}),$$

where the convergence is in the mean-square sense, uniformly in $\mathbf{x} \in \Omega$.

The random variables $\xi_j(\omega)$ are given by

$$(3.9) \quad \xi_j(\omega) = \frac{1}{\sqrt{\lambda_j}} \int_{\Omega} Z(\mathbf{x}, \omega) \phi_j(\mathbf{x}) d\mathbf{x}, \quad (\text{for } \lambda_j > 0)$$

and satisfy $\mathbb{E}[\xi_j] = 0$ and $\mathbb{E}[\xi_j \xi_m] = \delta_{jm}$ (Kronecker delta). If Z is a Gaussian random field, then the ξ_j are independent standard Gaussian random variables.

4. APPROXIMATION OF AUTOCOVARANCE FUNCTIONS VIA GAUSSIAN SUMS

Let $d = \|\mathbf{x} - \mathbf{y}\|_2$ denote the Euclidean distance between two points $\mathbf{x}, \mathbf{y} \in \mathbb{R}^D$. We consider stationary, isotropic autocovariance functions $C(d)$ defined for $d \geq 0$. For random fields in two or more dimensions D , it is highly desirable to express the autocovariance in a form that allows separation of individual dimensions, i.e.,

$$C(d) = \sum_{i=1}^k a_i \prod_{l=1}^D C_{il}(d_l^2), \quad d_l^2 = (x_l - y_l)^2.$$

Such a form of autocovariance will be very useful later for Galerkin discretization in subsection 5.2. We investigate the approximation of $C(d)$ using finite sums of Gaussian functions:

$$(4.1) \quad C_k(d) = \sum_{i=1}^k a_i e^{-b_i d^2}$$

where $a_i \in \mathbb{R}$ are coefficients of the basis functions and $b_i > 0$ are their scale parameters. Note that $d^2 = \sum_{l=1}^D d_l^2$ and therefore

$$e^{-b_i d^2} = \prod_{l=1}^D e^{-b_i d_l^2}, \quad \forall b_i.$$

4.1. General Approximability. We first establish the general conditions under which a function $C(d)$ can be approximated arbitrarily well by sums of the form (4.1) on a compact interval $[0, L]$ for some $L > 0$. This interval is typically chosen large enough to capture the significant decay of the covariance function. The natural space for measuring approximation error is often the Hilbert space $L^2(0, L)$ equipped with the norm $\|f\|_{L^2} = (\int_0^L |f(d)|^2 dd)^{1/2}$.

Theorem 4.1 (Stone–Weierstrass [28, Thm. 7.32]). *Let K be a compact interval $[0, L]$ for some $L > 0$ and let \mathcal{A} be an algebra of real-valued continuous functions on K ; that is, $\mathcal{A} \subset C([0, L])$ is closed under linear combinations and pointwise products. If*

- \mathcal{A} separates points: for every $x \neq y$ in K there exists $f \in \mathcal{A}$ with $f(x) \neq f(y)$, and
- \mathcal{A} vanishes at no point: for every $x \in K$ there exists $f \in \mathcal{A}$ with $f(x) \neq 0$,

then the uniform (supremum-norm) closure $\overline{\mathcal{A}}$ equals the whole space $C([0, L])$.

Proposition 4.2. *Let $V = \text{span}\{g_b(d) := e^{-bd^2} : b > 0\}$. Then, the vector space V is dense in the space of continuous functions $C([0, L])$ equipped with the supremum norm $\|\cdot\|_\infty$. Consequently, V is also dense in $L^2(0, L)$.*

Proof. We verify the assumptions of the Stone-Weierstrass theorem (theorem 4.1) for

$$\mathcal{A} := \text{span}\left(\{1\} \cup \{g_b : b > 0\}\right).$$

Clearly $V \subset \mathcal{A}$ and as $b \rightarrow 0$, $g_b(d) \rightarrow 1$, $\overline{V} = \overline{\mathcal{A}}$. So it suffices to show $\overline{\mathcal{A}} = C([0, L])$.

- \mathcal{A} is an algebra: Given finite sums $f = \sum_{i=1}^m a_i g_{b_i}$ and $h = \sum_{j=1}^n c_j g_{c_j}$, their product is

$$fh = \sum_{i,j} a_i c_j e^{-(b_i + c_j)d^2} \in \mathcal{A},$$

so \mathcal{A} is closed under pointwise multiplication (and, by being defined as span, also closed under addition and scalar multiplication).

- \mathcal{A} separates points: Let $x \neq y$ in $[0, L]$. Because $x^2 \neq y^2$, we have $g_b(x) = e^{-bx^2} \neq e^{-by^2} = g_b(y)$ for every $b > 0$. Hence a single $g_b \in \mathcal{A}$ distinguishes x and y .
- \mathcal{A} vanishes at no point: For any fixed $d \in [0, L]$ and any $b > 0$, $g_b(d) = e^{-bd^2} > 0$; thus every point has a non-zero value under every g_b , and in particular under some element of \mathcal{A} .

Then, by Stone-Weierstrass, supremum-norm closure $\overline{\mathcal{A}}$ equals $C([0, L])$. Since convergence in the supremum norm on $[0, L]$ implies convergence in the $L^2(0, L)$ norm (specifically, $\|f\|_{L^2} \leq \sqrt{L}\|f\|_\infty$), V is dense in $C([0, L])$ with the L^2 topology. As $C([0, L])$ is itself dense in $L^2(0, L)$, it follows by the triangle inequality that V is dense in $L^2(0, L)$. \square

This proposition guarantees that any autocovariance function $C(d)$ that is continuous on $[0, L]$ (and thus belongs to $L^2(0, L)$) can be approximated with arbitrary precision in the L^2 sense by a finite sum $C_k(d)$ as defined in (4.1).

4.2. Conditions for Non-Negative Coefficients. While Proposition 4.2 guarantees the existence of an approximation, it does not specify the signs of the coefficients a_i . However, we require the approximation of the autocovariance to be positive semidefinite; thus, the coefficients a_i must be positive. The sign structure of a_i is intimately linked to the concept of complete monotonicity.

Definition 4.3 (Complete Monotonicity). A function $f(x)$ defined on $(0, \infty)$ is *completely monotonic* if it is of class C^∞ and satisfies $(-1)^k f^{(k)}(x) \geq 0$ for all $x > 0$ and integers $k = 0, 1, 2, \dots$.

Bernstein's theorem provides an alternative definition of complete monotonicity of functions as Laplace transforms of non-negative measures, which will be very useful to link to the square exponential approximation.

Theorem 4.4 (Bernstein’s [33, Thm. 12a]). *A necessary and sufficient condition that $f(x)$ should be completely monotonic in $0 \leq x < \infty$ is that*

$$(4.2) \quad f(x) = \int_0^\infty e^{-xt} d\alpha(t),$$

where $\alpha(t)$ is bounded and non-decreasing and the integral converges for $0 \leq x < \infty$.

Now let $x = d^2$ and set $f(x) = C(\sqrt{x})$. Suppose f is completely monotone on $(0, \infty)$, or at least on $(0, L^2]$. By Bernstein’s theorem (Theorem 4.4), f admits the Laplace representation

$$(4.3) \quad C(d) = f(d^2) = \int_0^\infty e^{-d^2 t} d\mu(t),$$

where μ is a non-negative, bounded, and non-decreasing measure. The integral in (4.3) can be approximated by the finite Gaussian sum

$$(4.4) \quad C(d) \approx \sum_{i=1}^k w_i e^{-d^2 t_i}.$$

Because $\mu \geq 0$, it induces a bilinear form on the space of polynomials:

$$\langle p, q \rangle_\mu := \int_0^\infty p(t)q(t) d\mu(t).$$

If μ has infinite support, this form is strictly positive and thus defines an inner product on the space of polynomials. In that case, (4.4) can be interpreted as a Gaussian quadrature rule with nodes $b_i = t_i > 0$ and corresponding weights $a_i = w_i > 0$.

Classical error bounds for Gaussian quadrature with analytic integrands (see, e.g., [14, Ch. 2]) imply that the error in (4.4) decays *exponentially* with k . Hence the squared-exponential approximation should converge exponentially fast.

If μ is supported on finitely many points, $d\mu(t) = \sum_{i=1}^k w_i \delta_{t_i}(dt)$ with $a_i = w_i > 0$ and $b_i = t_i > 0$, then

$$C(d) = \sum_{i=1}^k a_i e^{-d^2 b_i},$$

so C is already a finite Gaussian mixture and no further approximation is necessary.

4.2.1. Non-negative coefficients for isotropic autocovariance functions. We now examine which *isotropic* autocovariance functions can be approximated by a mixture of Gaussians (squared-exponentials) with *non-negative* coefficients a_i in (4.1).

Theorem 4.5 (Schoenberg [29, Thm. 3], [32, Thm. 7.14]). *For a function $C: [0, \infty) \rightarrow \mathbb{R}$ the following two properties are equivalent:*

- (i) $C(\|x\|)$ is positive definite on every \mathbb{R}^D , $D \in \mathbb{N}$;
- (ii) the radial profile $C(\sqrt{\cdot})$ is completely monotone on $[0, \infty)$ and not constant.

Thus any isotropic kernel C that is positive definite in every dimension, including the Matérn, powered-exponential, Cauchy, and rational-quadratic families used throughout spatial statistics, has a completely monotone radial profile. Consequently, C admits the Bernstein-Widder representation (4.3). Restricting that integral to a bounded interval $[0, L]$ and replacing it by an k -point Gauss quadrature yields the finite Gaussian mixture (4.1) with weights $a_i = w_i > 0$ and nodes $b_i = t_i > 0$. The requirement $a_i > 0$ is therefore *not* an additional constraint, it

is the structural property that guarantees positive definiteness in every dimension and is automatically satisfied for all kernels of practical interest.

The only isotropic kernels that fail to be strictly positive definite are the degenerate cases (e.g. the constant kernel $C(d) \equiv \sigma^2$ or the identically zero kernel), which correspond to random fields with zero variance in some non-trivial linear combination of observations. Excluding these trivial exceptions, every isotropic covariance function encountered in practice fits naturally into the squared-exponential approximation framework with non-negative coefficients.

4.3. Numerical estimation of squared-exponential approximations. Let us focus on problems where the measure μ in (4.3) has infinite support. In principle, the exponents b_i could be chosen as the abscissae of a Gaussian quadrature rule for μ . However, the main challenge lies in the fact that the measure itself is *unknown*. We therefore adopt an optimization strategy to determine an optimal set of b_i for a given approximation rank k .

4.3.1. Problem setting. We approximate a one-dimensional covariance kernel by a non-negative sum of k squared-exponential terms

$$(4.5) \quad C(d) \approx \sum_{i=1}^k a_i e^{-b_i d^2}, \quad a_i > 0, \quad b_i > 0,$$

where $k \in \mathbb{N}$ is the *rank* of the approximation.

We consider the following five benchmark covariance kernels, all normalized to a unit length scale and defined over the domain $d \in [0, 2]$:

- Exponential kernel: $\exp(-d)$ [26];
- Matérn kernel ($\nu = \frac{5}{2}$): $C_{\frac{5}{2}}(d) = (1 + \sqrt{5}d + \frac{5}{3}d^2) \exp(-\sqrt{5}d)$ [30];
- Stretched exponential kernel: $\exp(-d^{0.6})$ [5];
- Rational-quadratic kernel: $(1 + d^2/2)^{-1}$ [26];
- Cauchy kernel: $\frac{1}{1 + d^2}$, a special case of the (generalized) Cauchy family [16].

This set spans exponential, algebraic, and heavy-tailed behaviors, posing various challenges for the finite-rank representation (4.5). We retain the domain $d \in [0, 2]$ because all pairwise distances that arise in subsequent experiments fall within this range. These experiments involve decomposing covariance functions on hypercubes $[0, 1]^D$, where $D = 1, 2, 3$. The maximum diameter of these domains is $\sqrt{3}$, which ensures that all relevant distances are encompassed by the chosen interval.

4.3.2. Optimization problem. Before formulating the optimization problem, we introduce a reparameterization that ensures the coefficients $b_i = e^{\theta_i}$ remain positive. In other words, we will optimize over the parameters θ_i instead. This reparameterization also addresses scaling issues, as the values of b_i grow exponentially, as demonstrated in subsequent experiments.

The continuous L^2 error is

$$\mathcal{J}(\mathbf{a}, \boldsymbol{\theta}) = \left\| \sum_{i=1}^k a_i e^{-e^{\theta_i} d^2} - f(d) \right\|_2 = \left[\int_0^2 \left(\sum_{i=1}^k a_i e^{-e^{\theta_i} d^2} - f(d) \right)^2 dd \right]^{1/2}, \quad b_i = e^{\theta_i}.$$

For computational practicality, the integral is approximated via numerical integration. In this context, we propose a *multi-level* Gauss-Legendre rule, i.e., a

composite rule consisting of Gauss–Legendre quadrature applied over multiple intervals. The multi-level structure partitions the interval $[0, L]$ into a sequence of subintervals: $[0, L\rho^m], [L\rho^m, L\rho^{m-1}], \dots, [L\rho^1, L]$, where $m \in \mathbb{N}$ denotes the number of levels and $\rho \in (0, 1)$ is the division ratio. This form of numerical quadrature is specifically designed to capture critical behavior near zero, particularly when b_i is large, as the squared-exponential kernel then requires fine resolution near zero for accurate approximation. Numerical experiments were conducted with $m = 5$, geometric ratio $\rho = 0.2$, and quadrature degree $n = 100$ on each subinterval, resulting in $(L + 1)n = 600$ nodes $(x_j, w_j)_{j=1}^{600}$. The corresponding discrete objective function is given by

$$J(\mathbf{a}, \boldsymbol{\theta}) = \left[\sum_{j=1}^{600} w_j \left(\sum_{i=1}^k a_i e^{-e^{\theta_i} x_j^2} - f(x_j) \right)^2 \right]^{1/2}.$$

Note that, due to the structure of the problem, the objective functionals $\mathcal{J}(\mathbf{a}, \boldsymbol{\theta})$ and $J(\mathbf{a}, \boldsymbol{\theta})$ possess multiple global minima, as the individual (b_i, a_i) pairs can be interchanged without affecting the value of the functional.

4.3.3. Optimization Algorithm. The unknowns are $\mathbf{p} = (\mathbf{a}, \boldsymbol{\theta}) \in \mathbb{R}^{2k}$, with non-negative $a_i \geq 0$ and unconstrained $\theta_i \in \mathbb{R}$. The non-negativity constraint is not enforced in the Newton algorithm, as the global minima are expected to naturally yield positive values. The minimization process is summarized as follows:

Newton–type iteration: At iteration \mathbf{p}_j , we compute the gradient ∇J_j and the Hessian H_j using JAX automatic differentiation (64-bit precision is necessary for stability). A damped Newton search direction \mathbf{s}_j is obtained from

$$(H_j + \tau_j I) \mathbf{s}_j = -\nabla J_j, \quad \tau_j \geq 0.$$

- (1) *Positive-definite case:* If $H_j + \tau_j I$ is positive definite, i.e., $\nabla J_j^\top \mathbf{s}_j < 0$ so that \mathbf{s}_j is a descent direction, set $\mathbf{d}_j = \mathbf{s}_j$ and decrease the damping parameter ($0 \leq \tau_{j+1} < \tau_j$).
- (2) *Indefinite case:* Otherwise, increase the damping ($\tau_{j+1} > \tau_j$) and fall back to steepest descent, $\mathbf{d}_j = -\nabla J_j$.

Line search: A backtracking line search on $[0, 1]$, using the golden-section ratio, determines the step length $\alpha_j \in (0, 1]$.

Update:

$$\mathbf{p}_{j+1} = \mathbf{p}_j + \alpha_j \mathbf{d}_j.$$

Stopping criteria: Terminate when

- (1) $\|\nabla J_j\|_2 < \varepsilon_\nabla$;
- (2) $\|\mathbf{p}_{j+1} - \mathbf{p}_j\|_2 < \varepsilon_\mathbf{p}$ for the last $n_\mathbf{p}$ iterations; or
- (3) the maximum iteration count is exceeded.

4.3.4. Initialization Strategy. The minimization of $J(\mathbf{a}, \boldsymbol{\theta})$ via Newton’s method is reliable only when the initial guess is sufficiently close to the minimizer; if it is too far, the iteration may diverge. Hence, one must employ either (i) a global search strategy or (ii) a *good* initial guess. We adopt the second approach because, thanks to the structure of the problem, such a guess can be reasonably estimated.

For a fixed rank k , the squared-exponential sum in (4.5) may be interpreted as a k -point quadrature rule for the Laplace–Stieltjes integral in (4.3), with *nodes* b_i and *weights* a_i . Gaussian quadrature minimizes the integration error among all rules

Algorithm 1 Initial guess $^{(0)}\theta_i^k$ for rank k

Require: maximum rank k_{\max}
Base ranks

- 1: $^{(0)}\theta_1^1 \leftarrow 0$
- 2: $^{(0)}\theta_1^2 \leftarrow * \theta_1^1 - 1, \quad ^{(0)}\theta_2^2 \leftarrow * \theta_1^1 + 1$

Ranks $k \geq 3$

- 3: **for** $k = 3$ **to** k_{\max} **do**
 - 4: $^{(0)}\theta_1^k \leftarrow * \theta_1^{k-1} + (* \theta_1^{k-1} - * \theta_1^{k-2})$
 - 5: $^{(0)}\theta_k^k \leftarrow * \theta_{k-1}^{k-1} + (* \theta_{k-1}^{k-1} - * \theta_{k-2}^{k-2})$
 - 6: **for** $i = 2$ **to** $k - 1$ **do**
 - 7: $r_i^k \leftarrow \begin{cases} \frac{1}{2}, & i = k - 1, k = 3, \\ r_{i-1}^k, & i = k - 1, k > 3 \\ r_i^k : * \theta_i^{k-1} = r_i^k * \theta_{i-1}^{k-2} + (1 - r_i^k) * \theta_i^{k-2}, & \text{otherwise} \end{cases}$
 - 8: $^{(0)}\theta_i^k \leftarrow r_i^k * \theta_{i-1}^{k-1} + (1 - r_i^k) * \theta_i^{k-1}$
 - 9: **end for**
 - 10: **end for**
-

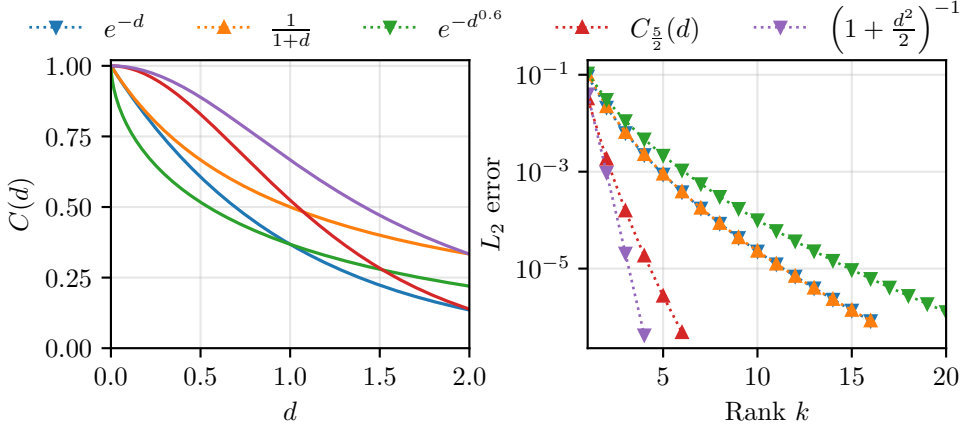


FIGURE 4.1. Left: Illustration of selected target kernels. Right: Approximation of the five target kernels by squared-exponential approximation with increasing rank size until $J(\mathbf{a}, \boldsymbol{\theta}) < 10^{-6}$.

with k nodes; therefore, the optimization problem is expected to recover the same node set. Denote the optimal exponents by $*b_i^k, i = 1, \dots, k$. Because the Gaussian nodes of consecutive orders alternate [14, Thm. 1.20], the optimal exponents are expected to satisfy

$$0 < *b_1^{k+1} < *b_1^k < *b_2^{k+1} < *b_2^k < \dots < *b_k^k < *b_{k+1}^{k+1}, \quad k \geq 1.$$

We exploit this property and additionally work with the log-transformed parameters $\theta_i = \log b_i$ to accommodate the exponential growth of b_i . Initial guesses $^{(0)}\theta_i^k$ that preserve the observed interior gap ratios are constructed as detailed in Algorithm 1. Once the θ_i have been initialized, the corresponding coefficients a_i are obtained via non-negative least squares (NNLS).

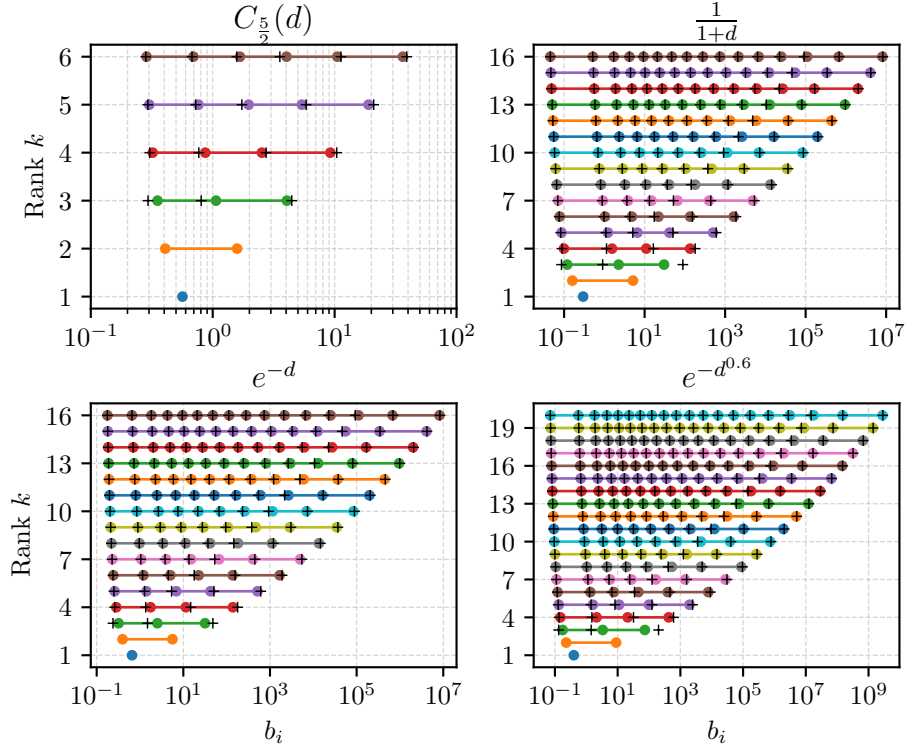


FIGURE 4.2. Optimal coefficients b_i for computed ranks for four selected kernels (black + signs illustrate the initial guesses).

kernel	$\varepsilon = 10^{-2}$		$\varepsilon = 10^{-3}$		$\varepsilon = 10^{-4}$		$\varepsilon = 10^{-6}$	
	k	exact ε	k	exact ε	k	exact ε	k	exact ε
e^{-d}	3	6×10^{-3}	5	9×10^{-4}	8	9×10^{-5}	16	8×10^{-7}
$C_{5/2}(d)$	2	2×10^{-3}	3	2×10^{-4}	4	2×10^{-5}	6	5×10^{-7}
$e^{-d^{0.6}}$	4	5×10^{-3}	7	6×10^{-4}	11	6×10^{-5}	20	1×10^{-6}
$(1 + d^2/2)^{-1}$	2	1×10^{-3}	2	1×10^{-3}	3	2×10^{-5}	4	4×10^{-7}
$1/(1 + d)$	3	6×10^{-3}	5	9×10^{-4}	8	9×10^{-5}	16	8×10^{-7}

TABLE 1. Ranks required to reach four target accuracies. Entries labeled "exact ε " show the actual achieved error for the reported rank.

4.3.5. *Experiments.* We combine the optimization algorithm of Section 4.3.3 with the initialization strategy of Section 4.3.4. Starting at rank $k = 1$, we increase the rank successively, with each converged solution providing the initial guess for the next run. The sequence terminates as soon as $J < 10^{-6}$; otherwise, it proceeds up to the upper limit $k_{\max} = 20$. All calculations are performed in double precision, which is required for the stable automatic differentiation used in computing the Hessians.

Figure 4.1 displays the five target kernels alongside their squared-exponential approximations for representative ranks. The plots reveal the expected exponential error decay, with a base rate that depends on each kernel’s rate of decay near $d = 0$. For subsequent demonstrations, we refer to an approximation by the tolerance ε that bounds its discrete L^2 error. The ranks required to achieve four tolerance levels, along with the corresponding errors, are listed in Table 1. Figure 4.2 shows the optimized exponents b_i alongside their initial guesses; the alternating property, approximate exponential growth, and the quality of the initial guesses are clearly evident.

5. NUMERICAL APPROXIMATION OF KARHUNEN–LOÈVE EXPANSION

Finding the exact eigenfunctions and eigenvalues of the autocovariance operator is, in most cases, impossible. Except for specific cases (e.g., exponential covariance on a one-dimensional interval), the eigenvalue problem (3.7) rarely admits an analytical solution. Therefore, numerical approximation methods are essential. We explore the use of Galerkin projection onto finite-dimensional subspaces spanned by orthonormal polynomials. Specifically, we consider tensor products of one-dimensional orthonormal polynomials, which are well-suited for hyper-rectangular domains.

5.1. Well-Posedness of the Spectral Eigenvalue Problem. The existence and properties of the KL expansion depend crucially on the spectral characteristics of the autocovariance operator \mathcal{C} defined in (3.6). It is necessary to ensure that the eigenvalue problem (3.7) is well-posed, i.e., that it admits a countable set of non-negative eigenvalues and corresponding orthonormal eigenfunctions.

Proposition 5.1. *Let $C(\mathbf{x}, \mathbf{y})$ be the autocovariance function of a zero-mean, second-order random field Z on the bounded domain Ω , and assume that C is continuous on $\Omega \times \Omega$. Then the integral operator $\mathcal{C} : L^2(\Omega) \rightarrow L^2(\Omega)$, defined by (3.6), is linear, bounded, self-adjoint, positive semi-definite, and compact.*

Proof. Linearity is immediate. Boundedness follows from the continuity of C on the compact set $\Omega \times \Omega$.

- **Self-adjointness:** Since $C(\mathbf{x}, \mathbf{y}) = \mathbb{E}[Z(\mathbf{x})Z(\mathbf{y})] = \mathbb{E}[Z(\mathbf{y})Z(\mathbf{x})] = C(\mathbf{y}, \mathbf{x})$, the kernel is symmetric. For any $f, g \in L^2(\Omega)$:

$$\langle \mathcal{C}f, g \rangle_{L^2(\Omega)} = \langle f, \mathcal{C}g \rangle_{L^2(\Omega)}.$$

- **Positive semi-definiteness:** For any $f \in L^2(\Omega)$:

$$\begin{aligned} \langle \mathcal{C}f, f \rangle_{L^2(\Omega)} &= \int_{\Omega} \int_{\Omega} \mathbb{E}[Z(\mathbf{x})Z(\mathbf{y})] f(\mathbf{y}) f(\mathbf{x}) d\mathbf{y} d\mathbf{x} \\ &= \mathbb{E} \left[\left(\int_{\Omega} Z(\mathbf{x}) f(\mathbf{x}) d\mathbf{x} \right)^2 \right] \geq 0. \end{aligned}$$

- **Compactness:** Since Ω is a bounded domain and C is continuous on $\Omega \times \Omega$, it is square-integrable: $\int_{\Omega} \int_{\Omega} |C(\mathbf{x}, \mathbf{y})|^2 d\mathbf{x} d\mathbf{y} < \infty$. Operators defined by such kernels (Hilbert–Schmidt integral operators) are compact on $L^2(\Omega)$ [12, Prop. 4.7].

□

The properties established in Proposition 5.1 allow us to invoke the Spectral Theorem for compact, self-adjoint operators on Hilbert spaces.

Theorem 5.2 (Spectral Theorem, Hilbert-Schmidt version [27], [20]). *Let $\mathcal{T} : H \rightarrow H$ be a compact, self-adjoint operator on a Hilbert space H . Then there exists a sequence of real eigenvalues $(\lambda_k)_{k=1}^\infty$ and an orthonormal sequence of corresponding eigenfunctions $(\phi_k)_{k=1}^\infty$ in H such that $\mathcal{T}\phi_k = \lambda_k\phi_k$. The sequence of eigenvalues converges to zero ($\lambda_k \rightarrow 0$ as $k \rightarrow \infty$), and the eigenfunctions form an orthonormal basis for $(\ker \mathcal{T})^\perp = \overline{\text{range } \mathcal{T}}$. Any $f \in H$ can be represented as*

$$f = \sum_{k=1}^{\infty} \langle f, \phi_k \rangle \phi_k + f_0,$$

where $f_0 \in \ker \mathcal{T}$, and

$$\mathcal{T}f = \sum_{k=1}^{\infty} \lambda_k \langle f, \phi_k \rangle \phi_k.$$

Applying Theorem 5.2 to the autocovariance operator \mathcal{C} , which is compact, self-adjoint, and positive semi-definite (Proposition 5.1), guarantees the existence of a countable sequence of non-negative eigenvalues $\lambda_k \geq 0$ with $\lambda_k \rightarrow 0$, and corresponding orthonormal eigenfunctions $\phi_k \in L^2(\Omega)$. This confirms that the eigenvalue problem (3.7), which defines the KL basis, is well-posed.

5.2. Tensor-product polynomial Galerkin approximation. As mentioned earlier, we work on the D -dimensional hyper-rectangle

$$\Omega = \prod_{l=1}^D (a_l, b_l) \subset \mathbb{R}^D,$$

as it permits the use of tensor-product orthonormal Legendre polynomials. For each coordinate $l = 1, \dots, D$, let

$$\{\varphi_\alpha^{(l)}\}_{\alpha \geq 0} \subset L^2((a_l, b_l))$$

denote the Legendre polynomials that are *orthonormal* on the interval (a_l, b_l) . For a multi-index $\alpha = (\alpha_1, \dots, \alpha_D) \in \mathbb{N}_0^D$ with $0 \leq \alpha_l \leq n$, we define the tensor-product basis functions

$$\psi_\alpha(\mathbf{x}) := \prod_{l=1}^D \varphi_{\alpha_l}^{(l)}(x_l), \quad \mathbf{x} = (x_1, \dots, x_D) \in \Omega.$$

Since each factor is orthonormal in its own coordinate, the set $\{\psi_\alpha\}$ forms an orthonormal basis of

$$V_n := \text{span}\{\psi_\alpha : 0 \leq \alpha_l \leq n\} \subset L^2(\Omega), \quad N_n := \dim V_n = (n+1)^D.$$

Let $\mathcal{C} : L^2(\Omega) \rightarrow L^2(\Omega)$ be the covariance operator of the random field under consideration. Its Galerkin projection $\mathcal{C}_n : V_n \rightarrow V_n$ is defined by

$$(5.1) \quad (\mathcal{C}_n u_n, v_n)_{L^2(\Omega)} := (\mathcal{C} u_n, v_n)_{L^2(\Omega)}, \quad u_n, v_n \in V_n.$$

With respect to the basis $\{\psi_\alpha\}$, this operator is represented by the symmetric, positive semi-definite matrix

$$A_n := [(\mathcal{C} \psi_\beta, \psi_\alpha)_{L^2(\Omega)}]_{\alpha, \beta} \in \mathbb{R}^{N_n \times N_n}.$$

The Galerkin approximation of the KL expansion is then defined by combining (3.7) and (5.1):

$$(\mathcal{C}\phi_j^{(n)}, v_n)_{L^2(\Omega)} = \lambda_j^{(n)} (\phi_j^{(n)}, v_n)_{L^2(\Omega)}, \quad \forall v_n \in V_n, j = 1, \dots, N_n.$$

With respect to the basis $\{\psi_\alpha\}$, this becomes the generalized eigenvalue problem $A_n \mathbf{u}_j^{(n)} = \lambda_j^{(n)} M_n \mathbf{u}_j^{(n)}$. Note that the mass matrix on the right-hand side is the identity, since the basis $\{\psi_\alpha\}$ is *orthonormal* in $L^2(\Omega)$. Therefore, the problem reduces to the matrix eigenvalue problem

$$(5.2) \quad A_n \mathbf{u}_j^{(n)} = \lambda_j^{(n)} \mathbf{u}_j^{(n)}, \quad \mathbf{u}_j^{(n)} \in \mathbb{R}^{N_n}, \lambda_j^{(n)} \geq 0.$$

Theorem 5.3. *For every $n \geq 0$, the problem (5.2) admits N_n real, non-negative eigenvalues*

$$0 \leq \lambda_{N_n}^{(n)} \leq \dots \leq \lambda_1^{(n)},$$

with corresponding $L^2(\Omega)$ -orthonormal eigenfunctions

$$\phi_j^{(n)} := \sum_{\alpha} u_{j,\alpha}^{(n)} \psi_{\alpha} \in V_n, \quad j = 1, \dots, N_n.$$

Hence, \mathcal{C}_n is diagonalizable, and the discrete KL expansion

$$X_n = \sum_{j=1}^{N_n} \sqrt{\lambda_j^{(n)}} \xi_j \phi_j^{(n)}, \quad \xi_j \stackrel{i.i.d.}{\sim} \mathcal{N}(0, 1)$$

is well-defined and forms a Gaussian random field with covariance kernel

$$C_n(\mathbf{x}, \mathbf{y}) := \sum_{j=1}^{N_n} \lambda_j^{(n)} \phi_j^{(n)}(\mathbf{x}) \phi_j^{(n)}(\mathbf{y}), \quad \mathbf{x}, \mathbf{y} \in \Omega.$$

5.3. Tensor-structured assembly of the Galerkin matrices. The squared-exponential representation derived in Section 4.3 yields a separable approximation of the isotropic covariance kernel:

$$\mathcal{C}(\mathbf{x}, \mathbf{y}) \approx C_{\text{sep}}(\mathbf{x}, \mathbf{y}) := \sum_{i=1}^k a_i \prod_{l=1}^D \exp(-b_i(x_l - y_l)^2), \quad a_i > 0, b_i > 0,$$

where D is the spatial dimension and k the separation rank. Together with the tensor-product Legendre basis $\{\psi_{\alpha}\}_{0 \leq \alpha_l \leq n}$ introduced in Section 5.2, the entries of the Galerkin matrix $A_n \in \mathbb{R}^{N_n \times N_n}$ (with $N_n = (n+1)^D$) are given by

$$(A_n)_{\beta, \alpha} = \iint_{\Omega \times \Omega} C_{\text{sep}}(\mathbf{x}, \mathbf{y}) \psi_{\alpha}(\mathbf{y}) \psi_{\beta}(\mathbf{x}) \, d\mathbf{y} \, d\mathbf{x}.$$

Because both the kernel and the basis are fully separable, each double integral factorizes into a product of one-dimensional integrals. Writing $\alpha = (\alpha_1, \dots, \alpha_D)$ and $\beta = (\beta_1, \dots, \beta_D)$, we obtain

$$(5.3) \quad (A_n)_{\beta, \alpha} = \sum_{i=1}^k a_i \prod_{l=1}^D \underbrace{\int_{a_l}^{b_l} \int_{a_l}^{b_l} e^{-b_i(x-y)^2} \varphi_{\alpha_l}^{(l)}(y) \varphi_{\beta_l}^{(l)}(x) \, dy \, dx}_{=:(\mathbf{A}_{n,i}^{(l)})_{\beta_l \alpha_l}}$$

where $\mathbf{A}_{n,i}^{(l)} \in \mathbb{R}^{(n+1) \times (n+1)}$ depends only on the polynomial degree n , the rank index i , and the spatial direction l . Consequently,

$$(5.4) \quad A_n = \sum_{i=1}^k a_i \bigotimes_{l=1}^D \mathbf{A}_{n,i}^{(l)}.$$

5.3.1. *Computational advantages.* The use of the squared-exponential approximation offers two main computational advantages:

- *Quadrature effort.* Direct assembly of A_n would require $N_n^2 = (n+1)^{2D}$ integrals over \mathbb{R}^{2D} . Formula (5.4) reduces this to $kD(n+1)^2$ integrals over *two-dimensional* domains, representing a dramatic saving even for moderate values of D .
- *Matrix-vector products.* Naively applying A_n to a vector of length N_n incurs a cost of $\mathcal{O}(N_n^2) = \mathcal{O}((n+1)^{2D})$ operations. By exploiting the tensor structure, this cost is reduced to $\mathcal{O}(kD(n+1)^{D+1})$.

Consider a realistic setting with polynomial degree $n = 100$ in $D = 2$ dimensions and a tensor sum with $k = 16$ terms. The naive cost of a matrix-vector multiplication grows as $\mathcal{O}((n+1)^{2D})$, which evaluates to about $101^4 \approx 10^8$ operations. In contrast, the cost of the tensor-structured approach scales as $\mathcal{O}(kD(n+1)^{D+1})$, which corresponds to approximately $16 \cdot 2 \cdot 101^3 \approx 3.3 \times 10^7$ operations. This results in roughly 3x speedup of matrix-vector multiplication.

The difference in integration cost is even more dramatic. Without separability, assembling A_n would require N_n^2 integrals over $2D$ dimensions. For $n = 100$ and $D = 2$, this corresponds to approximately 10^8 integrals over \mathbb{R}^4 . Using a tensor-product quadrature grid with 400 points per dimension, this would demand about $400^4 = 2.56 \times 10^{10}$ function evaluations per integral, totaling over 10^{18} evaluations. In contrast, the separated form involves only $kD(n+1)^2 \approx 3.3 \times 10^5$ integrals over \mathbb{R}^2 , each requiring only $400^2 = 1.6 \times 10^5$ function evaluations, for a total cost of approximately 5.2×10^{10} evaluations.

5.3.2. *Parity structure and block decomposition.* Additional speed-ups in the assembly, matrix-vector products, and final eigensolve are achieved by exploiting the *parity* of the Legendre basis functions appearing in the one-dimensional submatrices $\mathbf{A}_{n,i}^{(l)}$.

After shifting each spatial interval to be centered at the origin $(-\gamma, \gamma)$, the Legendre polynomials satisfy

$$\varphi_\alpha(-x) = (-1)^\alpha \varphi_\alpha(x), \quad \alpha = 0, 1, \dots, n.$$

Thus, φ_α is *even* when α is even and *odd* when α is odd.

For each kernel term in the separated covariance approximation, the one-dimensional factors introduced in (5.3) are given by

$$(\mathbf{A}_{n,i}^{(l)})_{\alpha\beta} = \int_{-\gamma}^{\gamma} \int_{-\gamma}^{\gamma} \exp(-b_i(x-y)^2) \varphi_\alpha(y) \varphi_\beta(x) dy dx, \quad 0 \leq \alpha, \beta \leq n, \quad i = 1, \dots, k.$$

Lemma 5.4 (parity orthogonality [7, 8]). *Let $p : [0, \infty) \rightarrow \mathbb{R}$, and let φ_{odd} and φ_{even} be odd and even functions, respectively, on $(-\gamma, \gamma)$. Then*

$$\int_{-\gamma}^{\gamma} \int_{-\gamma}^{\gamma} p(|x-y|) \varphi_{\text{odd}}(x) \varphi_{\text{even}}(y) dy dx = 0.$$

Taking $p(t) = \exp(-b_i t^2)$ in Lemma 5.4 yields

$$(\mathbf{A}_{n,i}^{(l)})_{\alpha\beta} = 0 \iff \alpha + \beta \text{ is odd.}$$

Permuting the basis so that the even degrees precede the odd degrees partitions each $\mathbf{A}_{n,i}^{(l)}$ into two diagonal blocks:

$$\mathbf{A}_{n,i}^{(l)} = \begin{bmatrix} \mathbf{A}_{n,i,\text{even}}^{(l)} & \mathbf{0} \\ \mathbf{0} & \mathbf{A}_{n,i,\text{odd}}^{(l)} \end{bmatrix}, \quad i = 1, \dots, k, \quad l = 1, \dots, D,$$

with $\mathbf{A}_{n,i,\text{even}}^{(l)} \in \mathbb{R}^{n_e \times n_e}$, $\mathbf{A}_{n,i,\text{odd}}^{(l)} \in \mathbb{R}^{n_o \times n_o}$, where $n_e = \lceil (n+1)/2 \rceil$ and $n_o = \lfloor (n+1)/2 \rfloor$.

Let

$$\epsilon = (\epsilon_1, \dots, \epsilon_D) \in \{0, 1\}^D, \quad \epsilon_l = 0 \text{ for even, } \epsilon_l = 1 \text{ for odd parity.}$$

Define the parity-specific factors

$$\mathbf{A}_{n,i}^{(l, \epsilon_l)} := \begin{cases} \mathbf{A}_{n,i,\text{even}}^{(l)}, & \epsilon_l = 0, \\ \mathbf{A}_{n,i,\text{odd}}^{(l)}, & \epsilon_l = 1. \end{cases}$$

After a global even/odd permutation P , the Galerkin matrix becomes block diagonal:

$$\tilde{A}_n := P^\top A_n P = \bigoplus_{\epsilon \in \{0,1\}^D} A_n^\epsilon, \quad A_n^\epsilon = \sum_{i=1}^k a_i \bigotimes_{l=1}^D \mathbf{A}_{n,i}^{(l, \epsilon_l)}.$$

Each block A_n^ϵ acts only on the tensor-product subspace spanned by basis functions with the prescribed parity vector ϵ . Its dimension is given by

$$N_\epsilon = \prod_{l=1}^D (n_e^{1-\epsilon_l} n_o^{\epsilon_l}) \leq \max\{n_e, n_o\}^D \approx \left(\frac{n+1}{2}\right)^D,$$

whereas the full space has dimension $N_n = (n+1)^D$. Thus, each block is smaller by a factor of approximately 2^D .

Because the blocks A_n^ϵ are mutually independent, the eigenproblems $A_n^\epsilon \mathbf{u} = \lambda \mathbf{u}$ can be solved separately and fully in parallel. One iteration of an Arnoldi-type routine, such as `eigs`, requires a single matrix–vector multiplication. For the *full* tensor matrix, this costs

$$\mathcal{O}(kD(n+1)^{D+1}) \quad (\text{see Section 5.3}).$$

After the parity permutation, the largest block has dimension $\left(\frac{n+1}{2}\right)^D$; consequently,

$$\mathcal{O}(kD((n+1)/2)^{D+1}) = \frac{1}{2^{D+1}} \mathcal{O}(kD(n+1)^{D+1}),$$

i.e., each block–matvec is 2^{D+1} times cheaper than the corresponding operation with the unsplit matrix, while there are only 2^D such blocks to process.

When the goal is to compute the leading $M2^D$ eigenpairs, one now computes M eigenpairs on each of the 2^D blocks, instead of computing $M2^D$ eigenpairs for the full matrix. Because Krylov and Arnoldi algorithms grow more than linearly in cost with the number of requested eigenpairs, this block-wise approach offers an additional practical acceleration beyond the formal factor of 2.

5.4. Stable quadrature for the one-dimensional blocks. The accurate evaluation of the matrices $\mathbf{A}_{n,i}^{(l)}$ in (5.3) is the final component that remains to be addressed. Although one can symbolically differentiate the Legendre polynomials and integrate them in closed form, the term $\exp(-b_i(x-y)^2)$ renders the computation numerically unstable, even for low polynomial orders, when $b_i \gg 1$. Instead, we rely on numerical quadrature, preceded by a coordinate transformation that broadens the narrow peak of the kernel. We demonstrate the approach on the reference square $[0, 1]^2$; however, generalization to any square is straightforward—for example, via an initial substitution into $[0, 1]^2$, which simply modifies b_i and introduces a multiplicative factor in the integral.

5.4.1. Duffy split and algebraic stretching. On the reference square $[0, 1]^2$, the kernel decays from 1 to e^{-1} once $|x - y| \gtrsim b_i^{-1/2}$. For large b_i , the informative part is confined to a thin strip around the diagonal $x = y$, so a naive tensor Gauss rule wastes almost all of its points.

The integral is first split along the diagonal,

$$\int_0^1 \int_0^1 F(x, y) dy dx = \int_0^1 \int_0^x F(x, y) dy dx + \int_0^1 \int_x^1 F(x, y) dy dx,$$

$$F(x, y) = e^{-b_i(x-y)^2} \phi_\alpha(x) \phi_\beta(y),$$

and each triangle is mapped back to the unit square by

$$(x, y) = (\xi, (1 - \eta)\xi) \quad \text{or} \quad (x, y) = (1 - \xi, (\eta - 1)\xi + 1), \quad (\xi, \eta) \in [0, 1]^2.$$

The Jacobian is ξ , and $(x - y)^2$ becomes $\xi^2 \eta^2$. Adding both contributions yields

$$\int_0^1 \int_0^1 \xi e^{-b_i \xi^2 \eta^2} \left[\phi_\alpha(\xi) \phi_\beta((1 - \eta)\xi) + \phi_\alpha(1 - \xi) \phi_\beta((\eta - 1)\xi + 1) \right] d\eta d\xi.$$

The peak is now restricted to the edges $\xi = 0$ and $\eta = 0$. As already shown, the integral is nonzero only for matching parity of ϕ_α and ϕ_β . Additionally, if the parity matches, we have $\phi_\alpha(x) = \phi_\alpha(1 - x)$ for even ϕ_α , and $\phi_\alpha(x) = -\phi_\alpha(1 - x)$ for odd ϕ_α , resulting in the simplification of the integral to

$$2 \int_0^1 \int_0^1 \xi e^{-b_i \xi^2 \eta^2} \phi_\alpha(\xi) \phi_\beta((1 - \eta)\xi) d\eta d\xi.$$

To distribute the peak from the edges over a larger portion of the square, we stretch those edges algebraically:

$$\xi = u^{g_x}, \quad \eta = v^{g_y}, \quad (u, v) \in [0, 1]^2,$$

with exponents $g_x, g_y \geq 1$. The resulting integral becomes

$$2 \int_0^1 \int_0^1 g_x g_y u^{g_x} v^{g_y} \exp(-b_i u^{2g_x} v^{2g_y}) \Theta_{\alpha\beta}(u^{g_x}, v^{g_y}) dv du,$$

where $\Theta_{\alpha\beta}$ contains the polynomial factors. Since we use this formulation to compute the entire matrix (i.e., the same maximal polynomial degree for both α and β), we may restrict ourselves to the same constant for both dimensions, $g = g_x = g_y$.

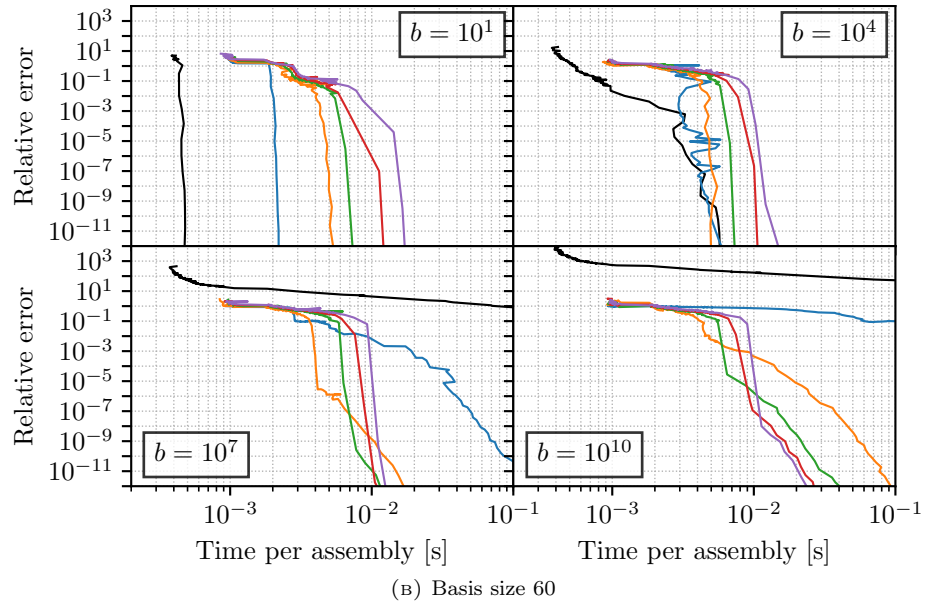
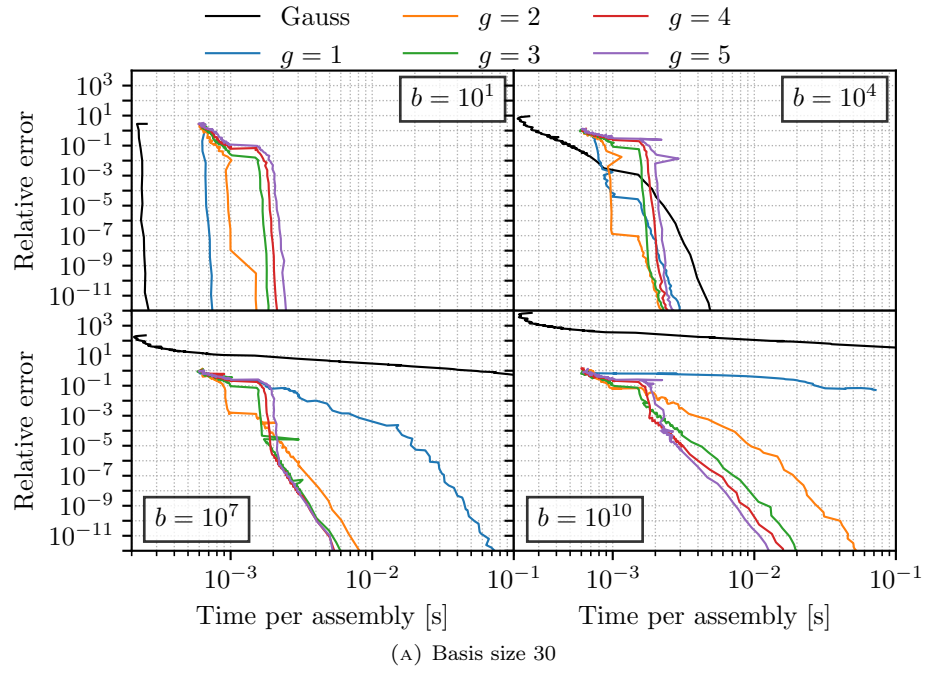


FIGURE 5.1. Efficiency of the proposed Duffy-based quadrature (color; algebraic exponents $g = 1 \dots 5$) compared to a standard tensor Gauss rule (black). Each panel corresponds to a different kernel coefficient b_i .

5.4.2. *Numerical experiment.* The algebraic stretching introduced above entails additional computational effort compared to a standard tensor Gauss rule. Each basis polynomial must now be evaluated at all points of the tensor grid, as its argument is $((1-\eta)\xi)$. This means we transition from a linear to a quadratic number of evaluation points, resulting in increased complexity when aggregating contributions.

To quantify the overall impact, we measured the time required to assemble a single matrix $\mathbf{A}_{n,i}^{(l)}$ (for 30/60 basis functions, i.e., up to polynomials of degree 29/59, evaluated separately for even and odd blocks) on an **AMD Ryzen 7 7735U** CPU using the vectorized `NumPy` and `opt_einsum` packages, along with an optimized BLAS/LAPACK build via the `blas-openblas` package. Figure 5.1 shows the resulting runtime versus the achieved relative Frobenius error of the assembled matrix for

$$b_i \in \{10^1, 10^4, 10^7, 10^{10}\}, \quad g \in \{1, 2, 3, 4, 5\},$$

alongside the reference tensor Gauss rule (black).

We observe the following:

- The plain Gauss rule is slightly faster for moderate values $b_i < 10^4$, as the kernel remains sufficiently broad. In this setting, the overhead from the transformation dominates.
- For each value of b_i , there exists an optimal value of g . Within the tested range, this optimal g varies from 2 to 5. In practice, values of b_i exceeding 10^{10} are uncommon, except in highly precise squared-exponential approximations. This is primarily because the stretching induced by high values of g also compresses regions farther from the axes, increasing the frequency of oscillating basis functions and, consequently, the number of quadrature points needed for accurate integration.
- Comparing the two basis sizes reveals similar overall behavior. For lower values of b_i , the reference tensor Gauss rule becomes marginally more efficient than the Duffy-based quadrature at higher polynomial degrees.

In summary, while the Duffy transformation introduces a modest overhead for wide kernels, it becomes essential once $b_i \gtrsim 10^4$. For the extreme localization characteristic of high-rank squared-exponential approximations ($b_i \geq 10^7$), the plain Gauss tensor product fails to achieve useful accuracy at a reasonable cost, whereas the proposed scheme remains both stable and efficient.

6. NUMERICAL EXPERIMENTS – 2-D SAMPLING

With the separable squared-exponential covariance fits from Section 4.3 and the tensor-product Legendre Galerkin discretisation introduced in Section 5.2, we computed truncated Karhunen-Loève expansions on the unit square $[0, 1]^2$ for all kernels listed in Subsection 4.3.1, along with the squared-exponential kernel e^{-d^2} . The parity block strategy from Section 5.3.2 enables efficient evaluation of the leading eigenpairs.

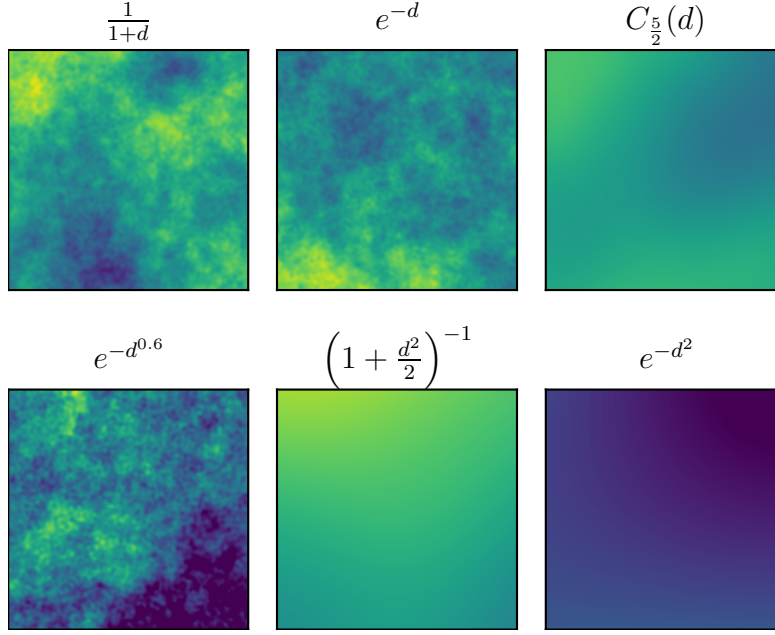


FIGURE 6.1. Random samples of the 2-D Gaussian fields on $[0, 1]^2$ for the benchmark kernels and their squared-exponential approximations (with precision 10^{-6}); see Table 1.

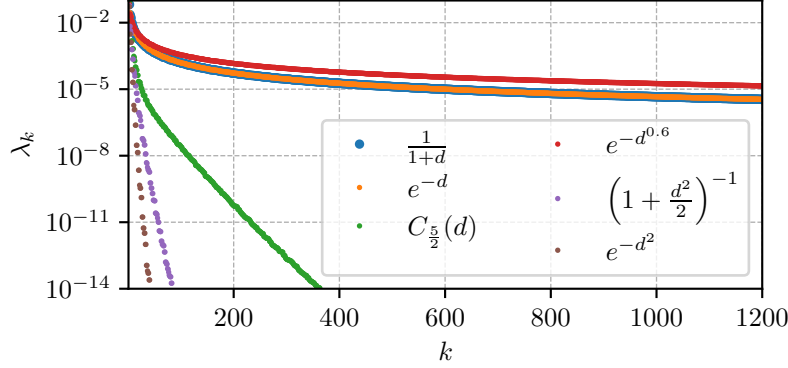


FIGURE 6.2. Eigenvalues of the 2-D KL expansion for the benchmark kernels and their squared-exponential approximations (with precision 10^{-6}); see Table 1.

To ensure accurate approximations of both samples and eigenvalues, we use the highest-precision squared-exponential fit, i.e., $\varepsilon = 10^{-6}$, with 150 basis functions in each dimension ($n = 149$), and compute the 1500 largest eigenvalues for each parity block. Figure 6.1 presents representative random-field realisations obtained by drawing independent standard Gaussian coefficients and summing the resulting KL series, while Figure 6.2 shows the numerically computed eigenvalues. A clear

relationship is evident between eigenvalue decay and the short-range correlation between points.

7. ACCURACY OF THE ONE-DIMENSIONAL KL APPROXIMATION

We conclude with a rough a posteriori error assessment of the KL discretisation. First, we consider the residual norm of an eigenpair approximation:

$$\mathcal{R}(u, \lambda) = \left\| \int_0^1 C(x, y) u(y) dy - \lambda u(x) \right\|_{L^2(0,1)},$$

evaluated via numerical quadrature (accounting for possible non-smoothness of the kernel at $x = y$). Second, we assess the error in reconstructing the covariance kernel:

$$\|C - C_N\|_{L^2([0,1]^2)} \quad \left(C_N(x, y) = \sum_{j=1}^N \lambda_j \phi_j(x) \phi_j(y) \right),$$

again computed via numerical quadrature, with care taken near the potential non-smoothness at $x = y$.

For both types of error estimation, we examine the effects of the squared-exponential approximation and the polynomial Galerkin approximation.

The numerical study is restricted to $\Omega = [0, 1]$, as the computational effort required to estimate $\mathcal{R}(u, \lambda)$ and $\|C - C_N\|_{L^2}$ becomes prohibitive in higher dimensions. However, the qualitative behaviour is expected to carry over to higher dimensions.

7.1. Residual decay of selected eigenpairs. Figure 7.1 shows the dependence of the residual error $\mathcal{R}(u_j, \lambda_j)$ on the polynomial degree of the Galerkin basis. It is presented for the 1st, 15th, and 30th eigenpairs of the exponential and Matérn ($\nu = \frac{5}{2}$) kernels, as the tolerance ε of the squared-exponential fit is refined (10^{-2} , 10^{-4} , 10^{-6}); see Table 1. For the dominant mode ($j = 1$), the residual decays exponentially until it reaches the plateau set by ε . Higher modes may already be at their lowest achievable error across all polynomial approximations, as their exact eigenvalues are smaller than ε ; see Table 2.

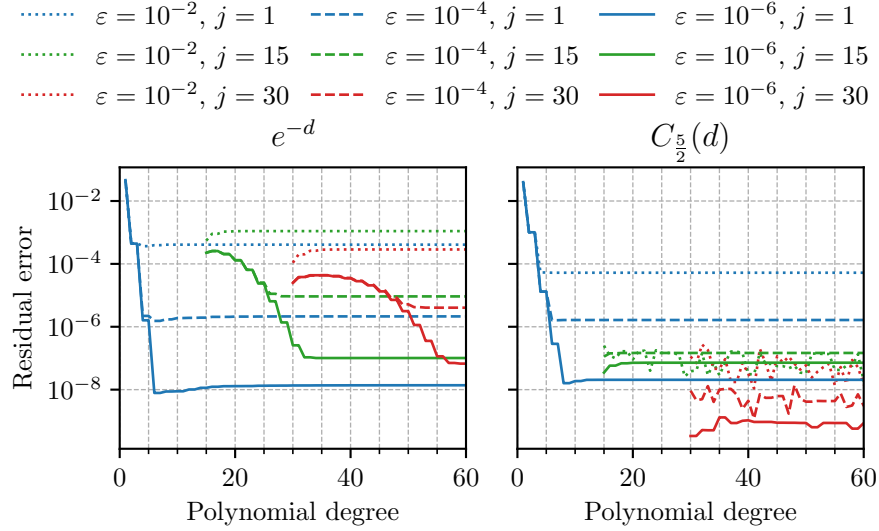


FIGURE 7.1. L^2 residual $\mathcal{R}(u_j, \lambda_j)$ for $j = 1, 15, 30$ under three squared-exponential tolerances $\varepsilon \in \{10^{-2}, 10^{-4}, 10^{-6}\}$; see Table 1.

TABLE 2. Exact eigenvalues corresponding to Figure 7.1. Values far below the fitting tolerance explain the instant convergence of the residual.

kernel	λ_1	λ_{15}	λ_{30}
exponential	7.388×10^{-1}	1.031×10^{-3}	2.409×10^{-4}
Matérn $\nu = \frac{5}{2}$	8.950×10^{-1}	3.210×10^{-9}	5.661×10^{-16}

7.2. Convergence of the truncated covariance. Figure 7.2 reports the error in reconstructing the covariance, $\|C - C_N\|_{L^2}$, for all five benchmark kernels as the degree of the polynomial Galerkin approximation increases. Two representative squared-exponential tolerances are used: $\varepsilon = 10^{-3}$ and 10^{-6} (see Table 1). Here, we use the full spectral decomposition—not just the largest eigenvalues, as this is feasible in the 1D case—to ensure that the estimate of $\|C - C_N\|_{L^2}$ remains accurate. The convergence rate closely follows the eigenvalue decay shown in Figure 6.2. Note that the results in the figure correspond to the 2D case.

An important observation can be made from the exponential kernel results in Figure 7.2. For kernels with slowly decaying eigenvalues, which require more squared-exponential terms to achieve a given ε , larger values of ε may still be acceptable—particularly when only a limited number of eigenvalues are needed. In such cases, the computed eigenpairs yield a similar approximation of C for both fine and coarse tolerances.

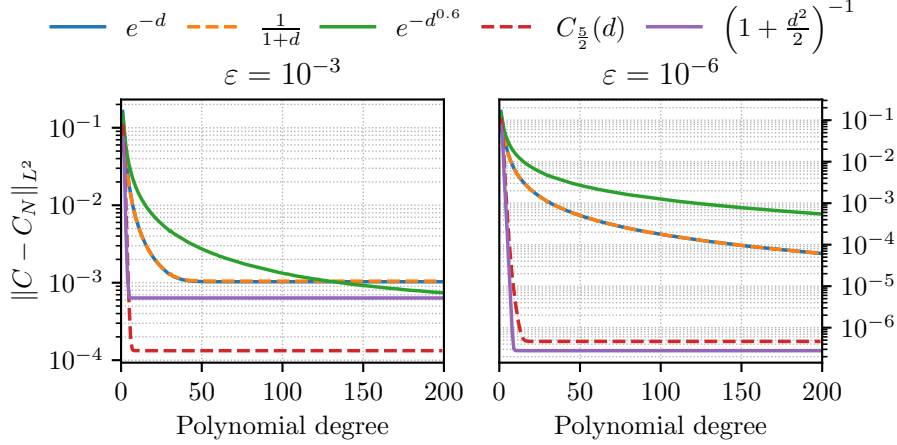


FIGURE 7.2. $\|C - C_N\|_{L^2}$ error of the truncated covariance C_N for $\varepsilon = 10^{-3}$ (left) and $\varepsilon = 10^{-6}$ (right); see Table 1.

8. CONCLUSIONS

The numerical approximation of the Karhunen-Loève expansion relies on orthogonal polynomials at several stages, making it natural to present both topics together in a single text. Section 2 demonstrates how the three-term recurrence relation for Legendre polynomials can be derived without resorting to differential equations or generating functions, thereby keeping the argument concise, clear, and accessible to undergraduates.

Sections 4 and 4.3 explain how every positive-definite isotropic covariance function can be expressed as an integral of squared-exponentials, and how a finite, non-negative squared-exponential approximation yields a close representation. Table 1 and Figure 4.1 illustrate that the approximation error decreases almost geometrically as the rank increases.

Given a separable kernel, Section 5.2 constructs a Legendre-Galerkin matrix that decomposes into Kronecker products of small one-dimensional blocks. Due to cancellation between even and odd Legendre modes, each block further splits, reducing both storage and computational effort in higher dimensions. The Duffy mapping with algebraic stretching, employed in Section 5.4, preserves quadrature stability even when the exponents in the squared-exponential approximation become very large; see Figure 5.1.

Figure 6.1 presents two-dimensional samples generated by the method, while Figure 6.2 displays the corresponding eigenvalues. Together, they demonstrate that the numerical scheme accurately captures both the spatial structure and spectral decay of the target fields.

All scripts to generate the tables and figures are available at https://github.com/Beremi/KL_decomposition, facilitating verification and reuse of the results with minimal effort.

REFERENCES

- [1] M. ABRAMOWITZ AND I. A. STEGUN, *Handbook of Mathematical Functions with Formulas, Graphs, and Mathematical Tables*, Dover Publications, New York, reprint of nbs 55 ed., 1965.

- [2] R. J. ADLER AND J. E. TAYLOR, *Random Fields and Geometry*, Springer Monographs in Mathematics, Springer, New York, 2007.
- [3] J. S. AZEVEDO, F. WISNIEWSKI, AND S. P. OLIVEIRA, *A galerkin method with two-dimensional haar basis functions for the computation of the Karhunen-Loève expansion*, Computational and Applied Mathematics, 37 (2018), pp. 1825–1846.
- [4] A. A. BASMAJI, M. M. DANNERT, AND U. NACKENHORST, *Implementation of Karhunen-Loève expansion using discontinuous legendre polynomial-based galerkin approach*, Probabilistic Engineering Mechanics, 67 (2022), p. 103176.
- [5] J. BERAN, *Statistics for Long-Memory Processes*, Chapman & Hall / CRC, New York, 1994.
- [6] W. BETZ, I. PAPAIOANNOU, AND D. STRAUB, *Numerical methods for the discretization of random fields by means of the Karhunen-Loève expansion*, Computer Methods in Applied Mechanics and Engineering, 271 (2014), pp. 109–129.
- [7] M. BÉRES, *Karhunen-loève decomposition of isotropic gaussian random fields using a tensor approximation of autocovariance kernel*, in High Performance Computing in Science and Engineering (HPCSE 2017), T. Kozubek, M. Čermák, P. Tichý, R. Blaheta, J. Šístek, D. Lukáš, and J. Jaroš, eds., vol. 11087 of Lecture Notes in Computer Science, Cham, 2018, Springer International, pp. 188–202.
- [8] ———, *Methods for the Solution of Differential Equations with Uncertainties in Parameters*, phd thesis, VŠB – Technical University of Ostrava, Ostrava, 2023.
- [9] T. S. CHIHARA, *An Introduction to Orthogonal Polynomials*, Gordon and Breach, New York, 1978. Reprinted by Dover, 2011.
- [10] J.-P. CHILÈS AND P. DELFINER, *Geostatistics: Modeling Spatial Uncertainty*, Wiley Series in Probability and Statistics, John Wiley & Sons, 2 ed., 2012.
- [11] G. CHRISTAKOS, *Random Field Models in Earth Sciences*, Academic Press, San Diego, 1992.
- [12] J. B. CONWAY, *A Course in Functional Analysis*, vol. 96 of Graduate Texts in Mathematics, Springer, New York, 2 ed., 1990.
- [13] A. R. FREEZE, *A stochastic-conceptual analysis of one-dimensional groundwater flow in nonuniform homogeneous media*, Water Resources Research, 11 (1975), pp. 725–741.
- [14] W. GAUTSCHI, *Orthogonal Polynomials: Computation and Approximation*, Numerical Mathematics and Scientific Computation, Oxford University Press, Oxford, 2004.
- [15] R. G. GHANEM AND P. D. SPANOS, *Stochastic Finite Elements: A Spectral Approach*, Springer-Verlag, New York, 1991.
- [16] T. GNEITING AND M. SCHLATHER, *Stochastic models that separate fractal dimension and the hurst effect*, SIAM Review, 46 (2004), pp. 269–282.
- [17] G. H. GOLUB AND C. F. VAN LOAN, *Matrix Computations*, Johns Hopkins University Press, Baltimore, 4 ed., 2013.
- [18] G. H. GOLUB AND J. H. WELSCH, *Calculation of gauss quadrature rules*, Mathematics of Computation, 23 (1969), pp. 221–230.
- [19] S. P. HUANG, S. T. QUEK, AND K. K. PHOON, *Convergence study of the truncated Karhunen-Loève expansion for simulation of stochastic processes*, International Journal for Numerical Methods in Engineering, 52 (2001), pp. 1029–1043.
- [20] E. KREYSZIG, *Introductory Functional Analysis with Applications*, John Wiley & Sons, New York, 1989.
- [21] Q. LIU AND X. ZHANG, *A Chebyshev polynomial-based galerkin method for the discretization of spatially varying random properties*, Acta Mechanica, 228 (2017), pp. 2063–2081.
- [22] M. LOÈVE, *Probability Theory II*, vol. 46 of Graduate Texts in Mathematics, Springer, New York, 4 ed., 1978.
- [23] M. L. MIKA, T. J. R. HUGHES, D. SCHILLINGER, P. WRIGGERS, AND R. R. HIEMSTRA, *A matrix-free isogeometric galerkin method for Karhunen-Loève approximation of random fields using tensor product splines, tensor contraction and interpolation-based quadrature*, Computer Methods in Applied Mechanics and Engineering, 379 (2021), p. 113730.
- [24] S. P. OLIVEIRA AND J. S. AZEVEDO, *Spectral element approximation of Fredholm integral eigenvalue problems*, Journal of Computational and Applied Mathematics, 257 (2014), pp. 46–56.
- [25] S. RAHMAN, *A galerkin isogeometric method for Karhunen-Loève approximation of random fields*, Computer Methods in Applied Mechanics and Engineering, 338 (2018), pp. 533–561.
- [26] C. E. RASMUSSEN AND C. K. I. WILLIAMS, *Gaussian Processes for Machine Learning*, MIT Press, Cambridge, MA, 2006.

- [27] M. REED AND B. SIMON, *Methods of Modern Mathematical Physics, Vol. 1: Functional Analysis*, Academic Press, New York, revised and enlarged ed., 1980.
- [28] W. RUDIN, *Principles of Mathematical Analysis*, McGraw-Hill, New York, 3 ed., 1976.
- [29] I. J. SCHOENBERG, *Metric spaces and completely monotone functions*, *Annals of Mathematics*, 39 (1938), pp. 811–841.
- [30] M. L. STEIN, *Interpolation of Spatial Data: Some Theory for Kriging*, Springer, 1999.
- [31] G. SZEGÖ, *Orthogonal Polynomials*, vol. 23 of American Mathematical Society Colloquium Publications, American Mathematical Society, Providence, RI, 4 ed., 1975.
- [32] H. WENDLAND, *Scattered Data Approximation*, vol. 17 of Cambridge Monographs on Applied and Computational Mathematics, Cambridge University Press, Cambridge, 2004.
- [33] D. V. WIDDER, *The Laplace Transform*, Princeton University Press, Princeton, 1941.
- [34] H. XIE AND T. ZHOU, *A multilevel finite element method for Fredholm integral eigenvalue problems*, *Journal of Computational Physics*, 303 (2015), pp. 173–184.

INSTITUTE OF GEONICS OF THE CAS, OSTRAVA, CZECH REPUBLIC

DEPARTMENT OF APPLIED MATHEMATICS, FACULTY OF ELECTRICAL ENGINEERING AND COMPUTER SCIENCE, VŠB – TECHNICAL UNIVERSITY OF OSTRAVA, OSTRAVA, CZECH REPUBLIC
 Email address: `michal.beres@vsb.cz`